Published in final edited form as:
Sci Immunol. ; 6(61): . doi:10.1126/sciimmunol.abg5003.

Pax5 regulates B cell immunity by promoting PI3K signaling via PTEN downregulation

Lesly Calderón[#1], **Karina Schindler**[#1], **Stephen G. Malin**[1,2], **Alexandra Schebesta**[1], **Qiong Sun**[1], **Tanja Schwickert**[1], **Chiara Alberti**[1], **Maria Fischer**[1], **Markus Jaritz**[1], **Hiromi Tagoh**[1,4], **Anja Ebert**[1,5], **Martina Minnich**[1], **Adrian Liston**[3], **Luisa Cochella**[1], **Meinrad Busslinger**[1,#]

[1]Research Institute of Molecular Pathology (IMP), Vienna Biocenter (VBC), Campus-Vienna-Biocenter 1, A-1030 Vienna, Austria

[2]Laboratory of Immunobiology, Department of Medicine Solna, Karolinska Institute, Stockholm, Sweden

[3]Laboratory of Lymphocyte Signalling and Development, The Babraham Institute, Cambridge CB22 3AT, UK

[#] These authors contributed equally to this work.

Abstract

The transcription factor Pax5 controls B cell development, but its role in mature B cells is largely enigmatic. Here, we demonstrated loss of Pax5 by conditional mutagenesis in peripheral B lymphocytes led to the significant reduction of B-1a, marginal zone (MZ) and germinal center (GC) B cells as well as plasma cells. Follicular (FO) B cells tolerated the loss of Pax5 but had a shortened half-life. The Pax5-deficient FO B cells failed to proliferate upon B cell receptor or toll-like receptor stimulation due to impaired PI3K-AKT signaling, which was caused by increased expression of PTEN, a negative regulator of the PI3K pathway. Pax5 restrained PTEN protein expression at the posttranscriptional level, likely involving *Pten*-targeting microRNAs. Additional PTEN loss in *Pten,Pax5* double-mutant mice rescued FO B cell numbers and the development of MZ B cells, but did not restore GC B cell formation. Hence, the posttranscriptional downregulation of PTEN expression is an important function of Pax5 that facilitates the differentiation and survival of mature B cells, thereby promoting humoral immunity.

[#]To whom correspondence should be addressed (Lead Contract): phone: (+43/1) 797 30 – 3150, fax: (+43/1) 797 30 – 223150, busslinger@imp.ac.at.
[4]Ludwig Institute for Cancer Research, University of Oxford, Oxford OX 7DQ, UK
[5]Department of Molecular Biology and Genetics, Aarhus University, Denmark

Author contributions: L.Calderón performed all cell proliferation and survival experiments, the rescue experiments with *Pten,Pax5* mutant mice, the respective phosflow and immunofluorescence experiments, the analysis of *miR29-a/b-1* mutant mice; K.S. performed the phosflow analysis of Pax5-deficient FO B cells, intracellular PTEN staining, RNA-seq analysis of anti-IgM-stimulated B cells and contributed to small-RNA-sequencing; S.G.M. performed the flow-cytometric analysis of mature B cell types, immunization experiments, H3K4me2 ChIP and RNA-seq analysis of anti-CD40 plus IL-4 activated B cells; A.S. analyzed the *Cd19*-Cre *Pax5*$^{fl/-}$ mice; Q.S. performed the BrdU experiments, ELISPOT assays and histological spleen analysis of immunized mice; T.S. provided advice on flow-cytometric and immunofluorescence analyses; C.A. performed the small-RNA-sequencing; H.T. generated the DHS-seq data; A.E. did the Pax5 Bio-ChIP-seq analysis of activated B cells; M.M. analyzed the bone marrow plasma cells; M.F. and M.J. performed the bioinformatic analysis of mRNA-seq, small-RNA-seq and ChIP-seq data; L.Cochella provided advice on microRNA experiments; A.L. provided the *miR29-a/b-1* $^{-/-}$ mouse; M.B. supervised the study and wrote the manuscript with L.Calderón.

Competing interests: The authors declare that they have no competing interests.

Keywords

Pax5; mature B cell types; class switch recombination; B cell receptor signaling; Toll-like receptor signaling; PI3K-AKT signaling; microRNA-mediated control of PTEN expression

Introduction

B cell immunity provides humoral protection against infections through the generation and secretion of high-affinity antibodies that recognize an almost unlimited diversity of pathogens. This enormous adaptive potential of B cells is generated through V(D)J recombination of the immunoglobulin heavy-chain (*Igh*) and light-chain (*Igk* and *Igl*) genes during early B cell development (1), which results in the emergence of immature B cells in the bone marrow. Upon migration to the spleen, these immature B cells differentiate into distinct mature B cell types present in peripheral lymphoid organs. The innate-like B-1a cells in the peritoneal and pleural cavities and the marginal zone (MZ) B cells in the spleen provide the first line of defense against pathogens by rapidly developing to antibody-secreting plasma cells in a T cell-independent manner (2, 3). In response to antigen stimulation and T cell help, follicular (FO) B cells in the spleen and lymph nodes differentiate into germinal center (GC) B cells that undergo class switch recombination (CSR) (4) and somatic hypermutation (SHM) (5) at immunoglobulin genes.

While CSR exchanges *Igh* constant (C_H) exon regions to generate IgH isotypes with distinct effector functions (4), SHM alters the antigen-binding variable (V) sequences of immunoglobulin heavy- and light-chains (5). Affinity-based selection in the GC subsequently leads to the clonal expansion of B cells expressing high-affinity B cell receptors, which then differentiate into proliferating, antibody-secreting plasmablasts (5). Upon migration to specialized bone marrow niches, plasmablasts differentiate into long-lived non-proliferating plasma cells secreting high amounts of antibodies (6). While these B cell responses are orchestrated by many transcription factors, we describe here the role of Pax5 in controlling these processes.

The transcription factor Pax5 (7) is an essential regulator of B cell commitment (8) and development (9), which is exclusively expressed in the B-lymphoid lineage within the hematopoietic system (10). At the molecular level, Pax5 fulfills a dual role in B lymphopoiesis as it acts as a transcriptional repressor to suppress B-lineage-inappropriate genes (11, 12) and as an activator to induce gene expression required for B cell development and function (12, 13). Pax5 regulates its gene expression program in part by inducing active chromatin at activated target loci and eliminating active chromatin at repressed target loci through recruitment of chromatin-remodeling and histone-modifying complexes (12, 14).

Pax5 is expressed throughout B cell development from pro-B cells in the bone marrow to mature B cells in peripheral lymphoid organs (10), where it is required for the generation of mature B cells (9). Pax5 maintains the B cell gene expression program also in mature B cells, as conditional inactivation of *Pax5* leads to the downregulation of B cell-specific genes and reactivation of lineage-inappropriate genes in these B cells (9, 11–13). Importantly, the conditional loss of Pax5 results in the conversion of mature B cells into functional T cells by

Europe PMC Funders Author Manuscripts

dedifferentiation to uncommitted progenitors in the bone marrow and, with progressing age of the mice, gives rise to the development of an aggressive progenitor cell leukemia (15). Hence, loss of the B cell phenotype upon *Pax5* inactivation highlights an important role of Pax5 in maintaining B cell identity throughout B lymphopoiesis (15, 16) and in suppressing B cell leukemia (15) in the mouse, which is consistent with its function as a haploinsufficient tumor suppressor in B cell acute lymphoblastic leukemia in humans (17).

In contrast to early B cell development, little is known about the role of Pax5 in controlling late B lymphopoiesis. Here, we used conditional *Pax5* inactivation in mature B cell types to demonstrate that B-1a, MZ B, GC B and plasma cells were not generated upon Pax5 loss. Pax5-deficient FO B cells had a shortened half-life, which was caused by impaired phosphoinositide 3-kinase (PI3K) signaling due to posttranscriptionally increased protein expression of PTEN, a negative regulator of the pathways. Our study therefore identified Pax5 as an essential regulator of different aspects of B cell immunity.

Results

Reduced numbers and shortened lifespan of follicular B cells lacking Pax5

To study the role of Pax5 in mature B cell types, we used the *Cd23*-Cre line, which initiates Cre-mediated recombination in immature B cells of the spleen (18), to delete the floxed (fl) exon 2 of *Pax5* (9) in control *Cd23*-Cre *Pax5* $^{fl/+}$ mice and *Cd23*-Cre *Pax5* $^{fl/-}$ littermates, which additionally contained the *Pax5* null (–) allele (19). Flow-cytometric analysis revealed a prominent CD21^{lo} B cell population (CD21^{lo}CD23^{hi}B220^{+}) in the spleen of *Cd23*-Cre *Pax5* $^{fl/-}$ mice instead of the CD21^{int} FO B cells (CD21^{int}CD23^{hi}B220^{+}) detected in control *Cd23*-Cre Pax5$^{fl/+}$ mice (Fig. 1A), consistent with the fact that Pax5 directly activates the *Cr2* (CD21) gene in mature B cells (9, 12). The *Pax5* mutant CD21^{lo} B cell population could reflect a differentiation arrest at an aberrant transitional B cell stage or correspond to Pax5-deficient FO B cells. As lymph nodes that lack transitional B cells (CD21^{-}CD23^{-}) contained only CD21^{lo}CD23^{hi} B cells in *Cd23*-Cre *Pax5* $^{fl/-}$ mice (Fig. 1B), we will herein refer to the CD21^{lo}CD23^{hi} B cell population as *Pax5* mutant FO B cells. These mutant FO B cells were reduced 3.5-fold in the spleen and 2.1-fold in the lymph nodes and mutants recirculating B cells were reduced 6.9-fold in the bone marrow of *Cd23*-Cre *Pax5* $^{fl/-}$ mice compared with *Cd23*-Cre *Pax5* $^{fl/+}$ mice (Fig. 1D). The upregulated expression of CD25, encoded by the repressed Pax5 target gene *Il2ra* (12), and the downregulated expression of IgD and CD21 in FO B cells of *Cd23*-Cre *Pax5* $^{fl/-}$ mice (Fig. 1A,B) suggested that Pax5 was lost in *Pax5* mutant FO B cells. Intracellular Pax5 staining confirmed the loss of Pax5 protein in all *Pax5* mutant FO B cells of the lymph node and in most of the *Pax5* mutant FO B cells of the spleen (Fig. 1E). This was further confirmed by the full deletion of the floxed *Pax5* exon 2 and an almost complete absence of the Pax5 protein in sorted *Pax5* mutant FO B cells, as revealed by PCR and immunoblot analyses, respectively (Fig. S1A,B). Hence, FO B cells were severely reduced in the absence of Pax5.

To investigate the lifespan of Pax5-deficient FO B cells, we continuously labeled *Cd23*-Cre *Pax5* $^{fl/-}$ and *Cd23*-Cre *Pax5* $^{fl/+}$ mice with the thymidine analogue bromodeoxyuridine (BrdU) for 10 days prior to flow-cytometric analysis of BrdU incorporation in FO B cells (Fig. 1F). BrdU was incorporated in 13.4% of all splenic FO B cells and 89.5% of all

Europe PMC Funders Author Manuscripts

immature B cells ($CD21^-CD23^-B220^+CD19^+$) in control *Cd23*-Cre *Pax5* $^{fl/+}$ mice (Figs. 1F and S1C), confirming that only a few immature B cells are integrated into the quiescent FO B cell pool during the 10-day labeling period (20). In contrast, 59% of the splenic FO B cells and 31% of the lymph node FO B cells in *Cd23*-Cre *Pax5* $^{fl/-}$ mice incorporated BrdU during the first 10 days (Fig. 1F), but were then efficiently replaced by unlabeled *Pax5* mutant FO B cells during the subsequent 15-day chase period in a manner similar to immature B cells (Figs. 1F and S1C). Moreover, short-term labeling for 2 hours demonstrated that the *Pax5* mutant FO B cells did not proliferate similar to control FO B cells (Fig. S1D). Together, these data revealed a shortened lifespan and rapid turnover of Pax5-deficient FO B cells in the spleen and lymph nodes. Expression of the pro-survival protein Bcl2 from the *Vav-Bcl2* transgene (21) could, however, not rescue the FO B cell numbers in the spleen and lymph nodes of *Vav-Bcl2 Cd23*-Cre *Pax5* $^{fl/-}$ mice (Fig. S1E).

Loss of B-1a and marginal zone B cells upon conditional *Pax5* inactivation

MZ B cells, which were defined as $B220^+CD21^{hi}CD23^{lo/-}$ or $B220^+CD1d^{hi}$ cells, were reduced 5.9- and 2.4-fold, respectively, in the spleen of *Cd23*-Cre *Pax5* $^{fl/-}$ mice compared with *Cd23*-Cre *Pax5* $^{fl/+}$ littermates (Fig. 1A,D). Consequently, few IgM^+ B cells were detected on histological spleen sections in the marginal zone outside of the MOMA-1$^+$ macrophage ring in B cell follicles of *Cd23*-Cre *Pax5* $^{fl/-}$ mice in contrast to *Cd23*-Cre *Pax5* $^{fl/+}$ mice (Fig. 1C). As expected, the MZ B cells of *Cd23*-Cre *Pax5* $^{fl/-}$ mice, which were defined by the Pax5-regulated marker CD21 ($B220^+CD21^{hi}CD23^{lo/-}$), did not upregulate CD25 expression (Fig. 1A) and retained the intact floxed *Pax5* allele (Fig. S1A), indicating that a sizeable fraction of MZ B cells did not delete *Pax5* (Fig. 1D). Intracellular Pax5 staining of the $B220^+CD1d^{hi}CD23^{lo/-}$ MZ B cells confirmed that 75% of the MZ B cells in the *Cd23*-Cre *Pax5* $^{fl/-}$ mice expressed the Pax5 protein at the same level as the MZ B cells of control littermates (Fig. 1E). Notably, 25% of MZ B cells lost Pax5 and downregulated CD21, but failed to accumulate (Fig. 1E), demonstrating that MZ B cells stringently depend on Pax5 function.

To study B-1a cells, we used the *Cd19*-Cre line, which initiates Cre-mediated recombination in early B cell development (22). Most B-1a cells ($IgM^{hi}CD5^+$) in the peritoneum of *Cd19*-Cre *Pax5* $^{fl/-}$ mice also expressed Pax5 at a normal level, consistent with efficient retention of the floxed *Pax5* allele, as opposed to the efficient *Pax5* deletion observed in B-1a cells of *Cd19*-Cre *Pax5* $^{fl/+}$ mice (Fig. 1G). Although 20% of the B-1a cells in *Cd19*-Cre *Pax5* $^{fl/-}$ mice were losing Pax5 expression, these cells did not accumulate, indicating that B-1a cells were lost upon *Pax5* inactivation. These data demonstrated that B-1a and MZ B cells did not tolerate the loss of Pax5.

Pax5-dependent initiation and maintenance of germinal center B cell differentiation

As Pax5 is already lost in *Cd23*-Cre *Pax5* $^{fl/-}$ FO B cells prior to germinal center (GC) B cell formation (Fig. 1E), we immunized *Cd23*-Cre *Pax5* $^{fl/-}$ and control *Cd23*-Cre *Pax5* $^{fl/+}$ mice with the T cell-dependent antigen NP-KLH (in alum) to study the role of Pax5 at the start of the GC B cell response. At day 7 after immunization, no GC B cells could be detected in the spleen of *Cd23*-Cre *Pax5* $^{fl/-}$ mice both by flow cytometry (Fig. 2A,B) and histological analysis (Fig. 2C).

Consistent with this result, no *Pax5*-deleted GC B cells were present in *Cd19*-Cre *Pax5* $^{fl/-}$ mice that were immunized for 10 days with sheep red blood cells (SRBCs; Fig. S2A-C). As *Aicda* (AID) and the *Aicda-Cre* transgene (18) are activated at an early phase of GC B cell differentiation (23), we assessed the function of Pax5 at subsequent stages of the GC B cell response by NP-KLH immunization of *Aicda*-Cre *Pax5* $^{fl/-}$ and control *Aicda*-Cre *Pax5* $^{fl/+}$ mice.

GC B cells in *Aicda*-Cre *Pax5* $^{fl/-}$ mice were significantly reduced at day 7 and 14 after immunization (Fig. 2D,E) and could not be detected on histological sections at day 14 (Fig. 2F). Importantly, GC B cells with complete deletion of the floxed *Pax5* allele were initially observed in the spleen of *Aicda*-Cre *Pax5* $^{fl/-}$ mice at day 5 after SRBC immunization, but were subsequently lost at day 8, as shown by flow-cytometric and histological analyses (Fig. S2D,E). Moreover, the differentiation of GC B cells in Peyer's patches, which are exposed to antigens of gastrointestinal microbiota, was also strongly impaired in *Aicda*-Cre *Pax5* $^{fl/-}$ mice (Fig. S2F).

Together, these data demonstrated an essential role of Pax5 in the initiation and maintenance of GC B cell differentiation. Moreover, NP-IgG1-specific memory B cells (NP $^{+}$IgG1^{+}CD38^{hi}CD19^{+}B220^{+}Lin^{-}) were absent in the spleen of *Aicda*-Cre *Pax5* $^{fl/-}$ mice at day 14 and 28 after NP-KLH immunization (Fig. S2G,H), indicating that IgG1^{+} memory B cells of GC-dependent or GC-independent origin were not generated upon conditional Pax5 loss in activated B cells.

Pax5 was required for the generation of plasma cells *in vivo*

Long-lived plasma cells (CD28^{+}CD138^{+}Lin^{-}) (11) in the bone marrow of non-immunized *Cd23*-Cre *Pax5* $^{fl/-}$ mice were 2.3-fold reduced compared with control *Cd23*-Cre *Pax5* $^{fl/+}$ mice (Fig. 2G,H) and retained the intact floxed *Pax5* allele (Fig. 2I), suggesting that they could be derived from MZ and B-1a cells, which failed to undergo *Pax5* deletion (Fig. 1E,G). Moreover, plasma cells secreting high-affinity or total NP-specific IgG1 antibodies were not detected by ELISPOT assay at day 7 and 14 after NP-KLH immunization in the spleen of *Cd23*-Cre *Pax5* $^{fl/-}$ and *Aicda*-Cre *Pax5* $^{fl/-}$ mice (Fig. 2J,L), respectively, consistent with the absence of high-affinity NP-specific IgG1 antibodies in the serum of *Cd23*-Cre *Pax5* $^{fl/-}$ mice (Fig. 2K). Hence, T cell-dependent B cell immune responses were effectively lost upon *Pax5* inactivation in mature B cells.

Pax5 regulated CSR, but not proliferation, upon anti-CD40 and IL-4 stimulation

To investigate whether Pax5 controls cell proliferation and class switch recombination (CSR), we stimulated CellTrace Violet-labeled FO B cells from lymph nodes of *Cd23*-Cre *Pax5* $^{fl/-}$ and *Cd23*-Cre *Pax5* $^{fl/+}$ mice with anti-CD40 and IL-4, which mimics T cell help. Consistent with the observed shortened lifespan (Fig. 1F), the viability of the Pax5-deficient B cells was greatly decreased relative to that of control B cells after 3 days of stimulation (Fig. 3A). The viable Pax5-deficient and control B cells diluted CellTrace Violet at a comparable frequency, resulting in a similar proliferation index for both cell types (Fig. 3A). Notably, the percentage of IgG1^{+} B cells at day 4 of stimulation was reduced 2.8-fold upon *Pax5* inactivation (Fig. 3B), demonstrating that Pax5 was required for efficient CSR to IgG1.

Europe PMC Funders Author Manuscripts

To study the molecular mechanism by which Pax5 controls CSR, we determined the genome-wide Pax5 binding (by ChIP-seq), DNase I hypersensitive (DHS) sites (by DHS-seq) and gene expression (by RNA-seq) in Pax5-deficient and control FO B cells after 2 days of anti-CD40 plus IL-4 stimulation (Fig. S3A-E and Table S1). Genes with important functions in CSR, base-excision repair, mismatch repair and non-homologous end joining were similarly expressed in stimulated Pax5-deficient and control B cells except for *Aicda*, encoding the central regulator AID of CSR and SHM (24), whose expression was 4-fold upregulated in the absence of Pax5 (Figs. 3C and S3G). Hence, the CSR defect in Pax5-deficient B cells was not caused by decreased expression of genes implicated in CSR or repair pathways.

The switch region located 5' of a constant gene exon is made accessible for CSR by germline transcription from an upstream I promoter that is activated by cytokine signaling (4, 25). The Iγ1 germline transcript (GLT) was strongly induced by anti-CD40 plus IL-4 stimulation in control B cells, whereas its expression was 2-fold reduced in Pax5-deficient B cells (Fig. 3D). The Cγ1 gene region contained Pax5-binding sites at the Iγ1 promoter and at a downstream enhancer known as Cγ1-2b DHS site 1 (26) (Fig. S3H). The DNase I hypersensitivity at the Iγ1 promoter and downstream enhancer was strongly reduced in stimulated Pax5-deficient B cells compared with control B cells (Fig. S3H) in contrast to the DHS sites at the control *Tbp* locus (Fig. S3I). These data therefore indicated that Pax5 promoted CSR to IgG1 by inducing the formation of open chromatin at the Iγ1 promoter and downstream enhancer.

Pax5 controlled B cell proliferation in response to BCR and TLR signaling

We next stimulated Pax5-deficient and control FO B cell by activating the Toll-like receptor 9 (TLR9) with CpG oligodeoxynucleotides and TLR4 with lipopolysaccharide (LPS) for 3 days, or the BCR with anti-IgM antibody and IL-4 for 4 days (Fig. 3E-G). The viability of Pax5-deficient B cells was greatly reduced relative to that of control B cells under all stimulation conditions (Fig. 3E-G). The viable Pax5-deficient B cells showed little dilution of CellTrace Violet, thus resulting in a strongly decreased proliferation index (Fig. 3E-G). As Pax5-deficient FO B cells undergo normal cell divisions upon anti-CD40 plus IL-4 treatment (Fig. 3A), we concluded that the loss of Pax5 did not affect IL-4 signaling and that the proliferation defect of Pax5-deficient FO B cells upon stimulation with anti-IgM and IL-4 must be caused by impaired BCR signaling. Together, these data revealed an essential role of Pax5 in the control of BCR and TLR signaling.

Impaired intracellular BCR and TLR signaling in the absence of Pax5

As TLR signaling results in MyD88-dependent activation of the transcription factor NF-κB (27), we investigated whether intracellular signaling leading to the degradation of the NF-κB inhibitor IκBα was impaired in Pax5-deficient FO B cells. As revealed by intracellular staining, IκBα was efficiently degraded in Pax5-deficient and control FO B cells within 15 min of CpG oligodeoxynucleotide addition or 60 min of LPS stimulation, indicating normal NF-κB activation in the absence of Pax5 (Fig. 4A). TLR signaling also engages the PI3K pathway (27), which depends on a crosstalk with BCR signaling in B cells (28, 29). While CpG-mediated TLR9 stimulation for 15 min did not induce phosphorylation of the signal

Europe PMC Funders Author Manuscripts

transducers BLNK and PLCγ2, it resulted in moderately increased SYK phosphorylation in Pax5-deficient and control FO B cells (Fig. 4B). In contrast, TLR9 signaling induced phosphorylation of AKT (at Thr308 and Ser473) and FOXO1,3 strongly in control FO B cells, but weakly in Pax5-deficient FO B cells (Figs. 4B and S4A). Hence, the loss of Pax5 did not affect NF-κB activation, but instead impaired PI3K signaling in response to TLR9 signaling.

Phosphorylation of AKT (at Thr308 and Ser473) and FOXO1,3 in response to anti-IgM stimulation of the BCR was also strongly impaired in Pax5-deficient FO B cells relative to control B cells (Figs. 4C and S4A). Moreover, phosphorylation of the 4E-BP1 and S6 proteins downstream of mTORC1 signaling was also affected (Fig. S4B), in agreement with a critical role of the PI3K-AKT pathway in controlling mTORC1 activity (30) (Fig. S4A). In contrast, the phosphorylation of SYK, BLNK and PLCγ2 was similarly increased in Pax5-deficient and control FO B cells upon anti-IgM treatment (Fig. 4C). Consistent with normal phosphorylation of these three signaling molecules, intracellular calcium mobilization (31) was efficiently induced in Pax5-deficient FO B cells in response to anti-IgM stimulation (Figs. 4D and S4A). The moderately attenuated calcium fluxes of the Pax5-deficient FO B cells could be explained by the loss of PI3K signaling, which minimally affects calcium signaling in anti-IgM-treated B cells (32). In summary, PI3K-AKT signaling, which is essential for cell proliferation and survival (30), was impaired in response to both TLR9 and BCR activation in Pax5-deficient FO B cells, while BCR-induced calcium signaling and TLR9-mediated NF-κB activation were largely normal in the absence of Pax5.

The genes coding for different components of the PI3K-AKT pathway were similarly expressed in Pax5-deficient and control FO B cells, except for *Cd19* coding for an essential upstream activator of the PI3K (33) (Fig. S4C). Pax5-deficient FO B cells in the lymph node and spleen expressed the CD19 protein at a 2.6- and 1.9-fold lower level relative to control B cells, respectively (Fig. S4D). Heterozygous *Cd19*$^{+/-}$ FO B cells with their 1.9-fold lower CD19 expression (Fig. S4D) could efficiently induce phosphorylation of AKT (S473) upon anti-IgM stimulation in contrast to the strongly impaired AKT phosphorylation observed in Pax5-deficient FO B cells (Fig. S4E). We therefore concluded that the lower expression of CD19 in Pax5-deficient FO B cells dud not explain the strong AKT signaling defect of these cells.

Pax5-dependent activation of immediate-early genes in response to BCR signaling

To investigate a role of Pax5 in controlling immediate-early gene activation, we performed RNA-seq analysis of FO B cells from lymph nodes of *Cd23*-Cre *Pax5*$^{fl/-}$ and *Cd23*-Cre *Pax5*$^{fl/+}$ mice before and after anti-IgM stimulation for 1 h (Fig. S5A-C and Table S2). The bioinformatic analysis of the RNA-seq data obtained at two time points of BCR stimulation and in B cells of two different genotypes (see Materials and Methods and Fig. S5D, E) resulted in the identification of 11 Pax5-independent and 39 Pax5-dependent immediate-early genes that were induced > 9-fold in control FO B cells (Fig. S5F and Table S3). The Pax5-independent and Pax5-dependent expression of immediate-early genes (Fig. 5A, B) was consistent with our finding that the intracellular signaling pathways of the BCR were either largely unaffected (SYK-BLNK-PLCγ2) or impaired (PI3K-AKT) in the absence of

Pax5 (Fig. 4C). Notably, 11 of the 39 Pax5-dependent immediate-early genes coded for known transcriptional regulators (Fig. 5C, D and Table S3). In summary, these data demonstrated that Pax5 directly or indirectly activated the expression of several transcription factors in response to BCR signaling.

miRNA-mediated downregulation of PTEN expression by Pax5 in mature B cells

As genes coding for essential components of PI3K-AKT signaling were not significantly regulated by Pax5 (Fig. S4C), we investigated the expression of the lipid phosphatase PTEN, which antagonizes the function of the phosphoinositide 3-kinase (PI3K) by converting phosphatidylinositol-3,4,5-triphosphate (PI(3,4,5)P_3) to PI(4,5)P_2 (30) (Fig. S4A). As shown by intracellular staining, PTEN protein expression was significantly increased in unstimulated Pax5-deficient FO B cells compared with control FO B cells, while phosphorylation of AKT (Ser473) was concomitantly reduced in the absence of Pax5 (Fig. 6A). *Pten* mRNA expression was, however, similar in FO B cells of both genotypes (Fig. 6A). PTEN expression is regulated at the posttranscriptional level by different microRNAs (miRNAs) that target the 3' untranslated region (3'UTR) of the *Pten* mRNA (34). To investigate whether the loss of miRNAs may cause the increased PTEN expression, we analyzed FO B cells lacking the RNase III enzyme Dicer, which is essential for processing of all pre-miRNAs to mature miRNAs (35). Importantly, Dicer-deficient (*Cd23*-Cre *Dicer1* $^{fl/fl}$) FO B cells expressed the PTEN protein at a similarly high level as Pax5-deficient FO B cells (Fig. 6B), although the *Pten* mRNA was not increased compared with control FO B cells (Fig. S6A). These data indicated that Pax5 may be involved in the generation of miRNAs that target the *Pten* mRNA.

As Pax5 did not regulate genes involved in the synthesis (Drosha, DGCR8 or Dicer) or function (Argonaute proteins) of miRNAs, we used small-RNA-sequencing (36) to determine the differential abundance of mature miRNAs in *Cd23*-Cre *Pax5* $^{fl/-}$ versus *Cd23*-Cre *Pax5* $^{fl/+}$ FO B cells from lymph nodes (Fig. 6C and Table S4) or spleen (Fig. S6B and Table S4). We next analyzed the miRNA dataset of lymph node FO B cells for differentially expressed *Pten*-targeting miRNAs according to the following criteria; a Pten-targeting miRNA should have a predicted 'total context++ score' (37) of < −0.47 (Fig. S6C) for targeting *Pten* 3'UTR sequences, should be part of the miRNAs accounting for 99% of the normalized read counts and should be differentially expressed with a P_{adj} value of < 0.05 (see Materials and methods). This analysis identified members of the miR-29, miR-26, miR-19 and miR-141 families as differentially expressed miRNAs, with strongly predicted *Pten* targeting, in lymph node FO B cells (Fig. 6C,D and Table S5). miRNAs of these four families were also differentially expressed in splenic FO B cells (Fig. S6B). Moreover, target sites in the *Pten* 3'UTR (Fig. 6D) have been experimentally validated for all four miRNA families; miR-19 (38), miR-26 (39), miR-29 (40–42) and miR-141 (43–45).

Of the *Pten*-targeting miRNAs, the four members of the miR-29 family were together most highly expressed (Figs. 6C and S6B) and were downregulated between 2.9- and 1.3-fold in Pax5-deficient FO B cells from lymph nodes and spleen (Fig. S6D). As the four miR-29 isoforms are encoded by the two loci *miR-29a/b-1* and *miR-29b-2/c,* we next analyzed the effect of deleting *miR-29a* and *miR-29b-1* on PTEN expression in FO B cells from lymph nodes of *miR-29a/b-1* $^{-/-}$ mice (46, 47). Intracellular staining revealed a small increase of PTEN expression in *miR-29a/b-1* $^{-/-}$ FO B cells compared with control FO B cells (Fig. 6E), while phosphorylation of AKT (S473) was reduced in *miR-29a/b-1* $^{-/-}$ FO B cells relative to control FO B cells upon anti-IgM stimulation (Fig. S6E). Given the small effect on PTEN expression in *miR-29a/b-1* $^{-/-}$ FO B cells, it is conceivable that the cumulative loss of other Pax5-deregulated *Pten*-targeting miRNAs (Table S5) may have contributed to the strongly increased PTEN expression observed in Pax5-deficient FO B cells. Together, these data indicated that Pax5 restrained PTEN expression in mature B cells, likely by controlling the abundance of *Pten*-targeting miRNAs.

Loss of PTEN rescued PI3K signaling and the survival of *Pax5* mutant FO B cells

To investigate whether the loss of PTEN may restore PI3K signaling in *Pax5* mutant FO B cells, we deleted the *Pten* gene in *Cd23*-Cre *Pax5* $^{fl/fl}$ *Pten* $^{fl/+}$ and *Cd23*-Cre *Pax5* $^{fl/fl}$ *Pten* $^{fl/fl}$ mice. Intracellular staining and immunoblot analyses revealed that the PTEN protein was lost in *Cd23*-Cre *Pax5* $^{fl/fl}$ *Pten* $^{fl/fl}$ FO B cells, while it was still expressed at elevated levels in *Cd23*-Cre *Pax5* $^{fl/fl}$ *Pten* $^{fl/+}$ FO B cells compared with control FO B cells (Fig. S7A,B). Anti-IgM stimulation for 15 min resulted in significantly increased phosphorylation of AKT (Ser473) in *Cd23*-Cre *Pax5* $^{fl/fl}$ *Pten* $^{fl/fl}$ FO B cells in contrast to *Cd23*-Cre *Pax5* $^{fl/fl}$ *Pten* $^{fl/+}$ FO B cells that exhibited the same low AKT phosphorylation levels as *Pax5* mutant FO B cells (Fig. 7A). Notably, FO B cell numbers were restored in lymph nodes of *Cd23*-Cre *Pax5* $^{fl/fl}$ *Pten* $^{fl/fl}$ mice in contrast to *Cd23*-Cre *Pax5* $^{fl/fl}$ *Pten* $^{fl/+}$ mice (Fig. 7B). Stimulation with CpG oligodeoxynucleotides, LPS or anti-CD40 and IL-4 for 3 days revealed that the survival of *Cd23*-Cre *Pax5* $^{fl/fl}$ *Pten* $^{fl/fl}$ FO B cells was rescued compared with *Cd23*-Cre *Pax5* $^{fl/fl}$ *Pten* $^{fl/+}$ FO B cells, while a partial rescue was observed upon anti-IgM plus IL-4 treatment for 4 days (Figs. 7C and S7C). The proliferation of *Cd23*-Cre *Pax5* $^{fl/fl}$ *Pten* $^{fl/fl}$ FO B cells was, however, not restored in response to stimulation with CpG, LPS or anti-IgM and IL-4 (Fig. S7C,D). Together, these data indicated that the combined loss of Pax5 and PTEN rescued PI3K signaling and cell survival, but not the proliferation of FO B cells.

Rescue of MZ B cell development in *Pten,Pax5* double-mutant mice

Splenic B cell numbers were partially restored in *Cd23*-Cre *Pax5* $^{fl/fl}$ *Pten* $^{fl/fl}$ mice (Fig. 7D,E). In contrast, GC B cells were present at very low numbers in the spleen of non-immunized *Cd23*-Cre *Pax5* $^{fl/fl}$ *Pten* $^{fl/fl}$ mice, while the residual GC B cells expressed normal Pax5 levels due to strong counterselection against *Pax5* deletion (Fig. S7E). Similarly, the numbers of GC B cells in Peyer's patches were low in *Cd23*-Cre *Pax5* $^{fl/fl}$ mice and increased in *Cd23*-Cre *Pax5* $^{fl/fl}$ *Pten* $^{fl/fl}$ mice, although Pax5 displayed normal expression in GC B cells of both genotypes (Fig. S7F). Hence, these data demonstrated that the loss of PTEN could not rescue the development of Pax5-deficient GC B cells.

To study MZ B cell differentiation, we took advantage of the fact that the higher expression of CD1d and TACI on MZ B cells compared with FO B cells could be used to distinguish these two cell types (Fig. S7G). MZ B cells ($CD19^+B220^+CD23^{lo/-}TACI^+CD1d^{hi}$) were present at similarly low abundance in *Cd23*-Cre *Pax5* $^{fl/fl}$ *Pten* $^{fl/+}$ mice as in *Cd23*-Cre *Pax5* $^{fl/fl}$ mice (Fig. 7D,F), and a major fraction of these residual MZ B cells failed to delete *Pax5* (Fig. 7D,G), thus indicating that the loss of one *Pten* allele did not restore MZ B cell

Europe PMC Funders Author Manuscripts

numbers. In marked contrast, the number of MZ B cells was 3.4-fold higher in *Cd23*-Cre *Pax5*$^{fl/fl}$ *Pten*$^{fl/fl}$ mice relative to *Pten*-expressing control mice, while MZ B cells were even more abundant in *Cd23*-Cre *Pten*$^{fl/fl}$ mice (Fig. 7D,F), confirming previous published work (48, 49). Notably, most MZ B cells (93%) in *Cd23*-Cre *Pax5*$^{fl/fl}$ *Pten*$^{fl/fl}$ mice did not express Pax5 and CD21, indicating that counterselection against *Pax5* deletion was no longer observed upon further PTEN loss (Fig. 7D,G). We therefore concluded that the additional loss of PTEN allowed Pax5-deficient B cells to differentiate to MZ B cells.

To confirm these results, we analyzed spleen sections from mice of all five genotypes by immunofluorescence analysis with antibodies detecting Pax5, IgM (B cells), MOMA-1 (metallophilic macrophages) or TCRβ (T cells; Fig. 8A). Staining with the anti-Pax5 antibody confirmed the loss of Pax5 in most B lymphocytes of *Cd23*-Cre *Pax5*$^{fl/fl}$, *Cd23*-Cre *Pax5*$^{fl/fl/}$ *Pten*$^{fl/+}$ and *Cd23*-Cre *Pax5*$^{fl/fl}$ *Pten*$^{fl/fl}$ mice (Fig. 8A). Moreover, MZ B cells located outside of the MOMA-1^{+} macrophage ring were largely absent in *Cd23*-Cre *Pax5*$^{fl/fl}$ and *Cd23*-Cre *Pax5*$^{fl/fl}$ *Pten*$^{fl/+}$ mice, but present in *Cd23*-Cre *Pax5*$^{fl/+}$, *Cd23*-Cre *Pten*$^{fl/fl}$ and *Cd23*-Cre *Pax5*$^{fl/fl}$ *Pten*$^{fl/fl}$ mice (Fig. 8A). We next measured the cellularity of the MZ B cell layer outside of the macrophage ring with a custom-made program (see Methods). This statistical evaluation corroborated that MZ B cell numbers were rescued only upon complete loss of PTEN in *Cd23*-Cre *Pax5*$^{fl/fl}$ *Pten*$^{fl/fl}$ mice (Figs. 8B and S7H). Together, these data demonstrated that the rescue of PI3K signaling in *Cd23*-Cre *Pax5*$^{fl/fl}$ *Pten*$^{fl/fl}$ mice restored MZ B cell development.

Discussion

Pax5 is a key regulator of B lymphocytes in health and disease, as it controls B cell lineage commitment (8), development (9) and identity (15), and functions as a prominent tumor suppressor (15, 17) or oncoprotein (50) in B cell leukemia. Here, we have studied the function of Pax5 in late B lymphopoiesis and demonstrated that the innate-like B-1 and MZ B cells stringently depended on this transcription factor, whereas FO B cells tolerated the loss of Pax5 but had a considerably shortened half-life. Immunization with T cell-dependent antigens revealed an essential role for Pax5 in the initiation and maintenance of GC B cell development and the subsequent generation of memory B cells and plasma cells. At the molecular level, Pax5 controlled PI3K signaling, which promoted the survival and proliferation of B cells upon BCR or TLR stimulation. The severe impairment of BCR and TLR signaling in response to adaptive and innate signals likely explains the loss of all mature B cell types in the absence of Pax5, which identifieed Pax5 as a central regulator of B cell immunity.

Here, we showed Pax5 was essential for efficient CSR to IgG1 by activating Iγ1 germline transcription by binding to and inducing open chromatin at the Iγ1 promoter and an enhancer located downstream of the Cγ1 gene. Pax5 was previously implicated in controlling CSR by binding to and activating the *Aicda* gene (51, 52), which encodes the essential CSR regulator AID (24). Unexpectedly, our genetic analysis revealed that *Aicda* expression in response to anti-CD40 plus IL-4 stimulation was strongly increased in Pax5-deficient FO B cells. While the transcription factor FOXO1 promotes CSR by activating *Aicda* expression (53, 54), its activity is negatively regulated through phosphorylation by the

Europe PMC Funders Author Manuscripts

AKT kinase (30) (Fig. S4A). Hence, Pax5 has two opposing effects on the regulation of CSR to IgG1. The loss of Pax5 directly interfered with Iγ1 promoter activity and indirectly led to increased *Aicda* expression by inhibiting PI3K signaling leading to enhanced FOXO1 activity. Notably, IgG1^{+} B cells were decreased rather than increased in the absence of Pax5, suggesting that the direct transcriptional effect on the Iγ1 promoter is dominant over the indirect posttranslational control leading to enhanced *Aicda* expression.

In contrast to the activation of CD40 and IL-4 receptor pathways, Pax5-deficient FO B cells failed to proliferate upon anti-IgM plus IL-4, LPS or CpG stimulation, thus revealing a severe impairment of BCR and TLR signaling in the absence of Pax5. Phosphorylation of signal transducers and analysis of intracellular calcium mobilization in response to BCR engagement demonstrated that Pax5-deficient FO B cells could efficiently activate the SYK-BLNK-PLCγ2-dependent calcium signaling pathway, which is essential for controlling B cell differentiation and cell fate decisions (31). Likewise, TLR signaling in Pax5-deficient FO B cells efficiently induced NF-κB activation via the MyD88 pathway, which stimulates pro-inflammatory cytokine gene expression (55). In contrast, signaling along the PI3K-AKT pathway, which is essential for cell proliferation and survival (30, 56), was severely impaired in Pax5-deficient FO B cells upon BCR or TLR stimulation. This common defect may explain the failure of Pax5-deficient FO B cells to proliferate in response to BCR or TLR signals. Consistent with this conclusion, B cells lacking the regulatory PI3K subunit p85a (*Pik3r1*) fail to proliferate in response to anti-IgM plus IL-4 treatment, but undergo normal proliferation upon anti-CD40 and IL-4 stimulation (57, 58), similar to our finding with Pax5-deficient FO B cells.

B-1a and MZ B cells stringently depend on PI3K signaling as they are lost in mice lacking the following positive regulators of this pathway: CD19 (59–61), the regulatory PI3K subunit p85a (*Pik3r1*) (57, 58), the catalytic PI3K subunit p110δ (*Pik3cd*) (32, 62) and both AKT1 and AKT2 (63). Moreover, *Akt1*$^{-/-}$ *Akt2*$^{-/-}$ mice have reduced numbers of splenic FO B cells and lose B-1a and MZ B cells (63), which resembles the *Pax5* mutant phenotype. In contrast, conditional loss of PTEN, a negative regulator of PI3K signaling, leads to hyperactivation of the pathway and thus to increased B-1a and MZ B cell development at the expense of FO B cell generation (48, 49, 62). Notably, the PI3K-AKT-FOXO1 signaling axis is essential for controlling the survival of mature B cells in response to 'tonic' BCR signaling (64). Consequently, the impaired PI3K signaling in the absence of Pax5 likely explains the loss of B-1 and MZ B cells as well as the shortened half-life of FO B cells.

While Pax5 did not transcriptionally regulate genes implicated in PI3K signaling including *Pten,* Pax5-deficient FO B cells exhibited significantly elevated expression of the PTEN protein, which antagonizes PI3K signaling by converting $PI(3,4,5)P_3$ to $PI(4,5)P_2$ (30). Expression of the PTEN protein is under posttranscriptional control by different miRNAs that target the *Pten* 3'UTR (34). Our observation that the PTEN protein levels were equally high in Dicer- and Pax5-deficient FO B cells strongly suggests a role for Pax5 in the control of miRNA expression, although genes implicated in miRNA processing or function are not deregulated by Pax5. By small-RNA-seq, we identified four distinct *Pten*-targeting miRNA families (miR-29, miR-26, miR-19 and miR-141), whose abundance was deregulated in Pax5-deficient versus Pax5-expressing FO B cells. Interestingly, the four miRNAs of the

Europe PMC Funders Author Manuscripts

miR-29 family were not only abundantly expressed in FO B cells, but were also present at a 2.9- to 1.3-fold lower abundance in Pax5-deficient FO B cells relative to control B cells in the spleen and lymph nodes. However, loss of miR-29a and miR-29b-1 led only to a small increase of PTEN expression and concomitant decrease of AKT phosphorylation in FO B cells of *miR-29a/b-1* $^{-/-}$ mice. A significant loss of mature B cells and plasma cells was recently reported upon deletion of both the *miR-29a/b-1* and *miR-29c/b-2* loci, although deletion of all four *miR-29* genes still resulted in a modest increase of PTEN expression (65). It is thus conceivable that the cumulative loss of other Pax5-regulated *Pten*-targeting miRNAs may have contributed to the high PTEN expression observed in Pax5-deficient FO B cells. While we detected robust Pax5 binding at the *miR-29* loci, future experiments will be required to address whether Pax5 directly controls expression of the primary miRNA transcripts or indirectly determines the abundance of the mature miRNAs.

Additional loss of PTEN restored AKT phosphorylation and cell survival in *Pten,Pax5* double-mutant FO B cells in response to BCR and TLR stimulation. However, *in vitro* B cell proliferation was not rescued, suggesting that Pax5 may, in addition to its effect on PI3K signaling, activate genes implicated in cell cycle entry or progression, as exemplified by the immediate-early genes *Myc, Egr2* and *Egr3,* which are essential for antigen-induced B cell proliferation (66, 67). Nevertheless, FO B cell numbers were restored in the lymph nodes, and MZ B cells were rescued and properly located in the marginal zone of lymphoid follicles in the spleen of *Pten,Pax5* double-mutant mice. As the B cell-specific loss of PTEN alone already increases MZ B cell development (48, 49, 62), two different scenarios might explain the MZ B cell rescue in *Pten,Pax5* double-mutant mice. First, in addition to controlling PI3K signaling, Pax5 may fulfill another essential function to promote MZ B cell development. In this case, PTEN loss should only rescue the majority of the residual MZ B cells that fail to delete *Pax5* in *Cd23*-Cre *Pax5* $^{fl/fl}$ mice. Second, the main function of Pax5 in MZ B cell generation may be to restrain PTEN protein expression to promote PI3K signaling. In this scenario, the Pax5-deleted MZ B cells, which are prone to die, should be rescued by PTEN loss, thus giving rise to increased MZ B cell development. Our observation that the majority of rescued MZ B cells in *Pten,Pax5* double-mutant mice have lost Pax5 strongly indicates that the loss of PTEN can rescue the *Pax5* mutant phenotype, as Pax5 and PTEN fulfill opposing roles in controlling PI3K signaling and MZ B cell development.

Our study furthermore demonstrated that Pax5 was essential for the initiation and maintenance of GC B cell differentiation. At the start of this developmental process, quiescent FO B cells are activated by antigen-mediated stimulation of the BCR and by interaction with T helper cells, which triggers a cascade of events leading to the formation of GC B cells (68). As BCR activation starts this process, it is conceivable that quiescent FO B cells lacking Pax5 may fail to initiate efficient B cell activation due to impaired PI3K signaling. However, GC B cells are generated upon B cell-specific loss of PTEN (48, 53) or the catalytic PI3K subunit p110δ (69). Hence, PI3K signaling does not play an essential role in the generation of GC B cells, which likely explains why GC B cells cannot be rescued upon additional loss of PTEN in *Pten,Pax5* double-mutant mice. Pax5 must therefore regulate GC B cell differentiation through another important, yet unknown, function possibly involving Pax5-mediated control of cell proliferation.

Europe PMC Funders Author Manuscripts

In summary, although the pleiotropic transcription factor Pax5 controls many genes (12) (this study) and may thus contribute to the regulation of diverse aspects of B cells, we have shown here that the posttranscriptional downregulation of PTEN expression is an important function of Pax5 in mature B cells. As a consequence, Pax5 facilitates PI3K signaling leading to the differentiation and survival of distinct mature B cell types, which jointly cooperate to provide humoral immunity.

Supplementary Material

Refer to Web version on PubMed Central for supplementary material.

Acknowledgements

We thank Karin Aumayr's team for flow-cytometric sorting, Thomas Lendl for image analysis and Andreas Sommer's team at the Vienna BioCenter Core Facilities for Illumina sequencing.

Funding

This research was funded by Boehringer Ingelheim, the European Research Council under the European Union's Horizon 2020 research and innovation program (grant agreements 291740-LymphoControl and 740349-PlasmaCellControl), the Austrian Research Promotion Agency (Early Stage Grant 'Molecular Control' FFG-878286) and the Human Frontier Science Program fellowship LT00427/2013 (to L. Calderón).

Data and materials availability

RNA-seq, ChIP-seq, DHS-seq and small-RNA-seq data, which were generated for this study (Table S6), are available at the Gene Expression Omnibus (GEO) repository under the accession number GSE103260. All data needed to evaluate the conclusions in the paper are present in the paper of the Supplementary Material.

References and Notes

1. Bassing CH, Swat W, Alt FW. The mechanism and regulation of chromosomal V(D)J recombination. Cell. 2002; 109:S45–S55. [PubMed: 11983152]
2. Baumgarth N. The double life of a B-1 cell: self-reactivity selects for protective effector functions. Nat Rev Immunol. 2011; 11:34–46. [PubMed: 21151033]
3. Cerutti A, Cols M, Puga I. Marginal zone B cells: virtues of innate-like antibody-producing lymphocytes. Nat Rev Immunol. 2013; 13:118–132. [PubMed: 23348416]
4. Chaudhuri J, Alt FW. Class-switch recombination: interplay of transcription, DNA deamination and DNA repair. Nat Rev Immunol. 2004; 4:541–552. [PubMed: 15229473]
5. Victora GD, Nussenzweig MC. Germinal centers. Annu Rev Immunol. 2012; 30:429–457. [PubMed: 22224772]
6. Nutt SL, Hodgkin PD, Tarlinton DM, Corcoran LM. The generation of antibody-secreting plasma cells. Nat Rev Immunol. 2015; 15:160–171. [PubMed: 25698678]
7. Cobaleda C, Schebesta A, Delogu A, Busslinger M. Pax5: the guardian of B cell identity and function. Nat Immunol. 2007; 8:463–470. [PubMed: 17440452]
8. Nutt SL, Heavey B, Rolink AG, Busslinger M. Commitment to the B-lymphoid lineage depends on the transcription factor Pax5. Nature. 1999; 401:556–562. [PubMed: 10524622]
9. Horcher M, Souabni A, Busslinger M. Pax5/BSAP maintains the identity of B cells in late B lymphopoiesis. Immunity. 2001; 14:779–790. [PubMed: 11420047]

10. Fuxa M, Busslinger M. Reporter gene insertions reveal a strictly B lymphoid-specific expression pattern of *Pax5* in support of its B cell identity function. J Immunol. 2007; 178:3031–3037. [PubMed: 17312149]
11. Delogu A, et al. Gene repression by Pax5 in B cells is essential for blood cell homeostasis and is reversed in plasma cells. Immunity. 2006; 24:269–281. [PubMed: 16546096]
12. Revilla-i-Domingo R, et al. The B-cell identity factor Pax5 regulates distinct transcriptional programmes in early and late B lymphopoiesis. EMBO J. 2012; 31:3130–3146. [PubMed: 22669466]
13. Schebesta A, et al. Transcription factor Pax5 activates the chromatin of key genes involved in B cell signaling, adhesion, migration, and immune function. Immunity. 2007; 27:49–63. [PubMed: 17658281]
14. McManus S, et al. The transcription factor Pax5 regulates its target genes by recruiting chromatin-modifying proteins in committed B cells. EMBO J. 2011; 30:2388–2404. [PubMed: 21552207]
15. Cobaleda C, Jochum W, Busslinger M. Conversion of mature B cells into T cells by dedifferentation to uncommitted progenitors. Nature. 2007; 449:473–477. [PubMed: 17851532]
16. Mikkola I, Heavey B, Horcher M, Busslinger M. Reversion of B cell commitment upon loss of *Pax5* expression. Science. 2002; 297:110–113. [PubMed: 12098702]
17. Mullighan CG, et al. Genome-wide analysis of genetic alterations in acute lymphoblastic leukaemia. Nature. 2007; 446:758–764. [PubMed: 17344859]
18. Kwon K, et al. Instructive role of the transcription factor E2A in early B lymphopoiesis and germinal center B cell development. Immunity. 2008; 28:751–762. [PubMed: 18538592]
19. Urbánek P, Wang Z-Q, Fetka I, Wagner EF, Busslinger M. Complete block of early B cell differentiation and altered patterning of the posterior midbrain in mice lacking Pax5/BSAP. Cell. 1994; 79:901–912. [PubMed: 8001127]
20. Rolink AG, Andersson J, Melchers F. Characterization of immature B cells by a novel monoclonal antibody, by turnover and by mitogen reactivity. Eur J Immunol. 1998; 28:3738–3748. [PubMed: 9842916]
21. Ogilvy S, et al. Constitutive Bcl-2 expression throughout the hematopoietic compartment affects multiple lineages and enhances progenitor cell survival. Proc Natl Acad Sci USA. 1999; 96:14943–14948. [PubMed: 10611317]
22. Rickert RC, Roes J, Rajewsky K. B lymphocyte-specific, Cre-mediated mutagenesis in mice. Nucleic Acids Res. 1997; 25:1317–1318. [PubMed: 9092650]
23. Muramatsu M, et al. Specific expression of activation-induced cytidine deaminase (AID), a novel member of the RNA-editing deaminase family, in germinal center B cells. J Biol Chem. 1999; 274:18470–18476. [PubMed: 10373455]
24. Muramatsu M, et al. Class switch recombination and hypermutation require activation-induced cytidine deaminase (AID), a potential RNA editing enzyme. Cell. 2000; 102:553–563. [PubMed: 11007474]
25. Stavnezer J, Guikema JEJ, Schrader CE. Mechanism and regulation of class switch recombination. Annu Rev Immunol. 2008; 26:261–292. [PubMed: 18370922]
26. Medvedovic J, et al. Flexible long-range loops in the V_H gene region of the *Igh* locus facilitate the generation of a diverse antibody repertoire. Immunity. 2013; 39:229–244. [PubMed: 23973221]
27. Rawlings DJ, Schwartz MA, Jackson SW, Meyer-Bahlburg A. Integration of B cell responses through Toll-like receptors and antigen receptors. Nat Rev Immunol. 2012; 12:282–294. [PubMed: 22421786]
28. Otipoby KL, et al. The B-cell antigen receptor integrates adaptive and innate immune signals. Proc Natl Acad Sci USA. 2015; 112:12145–12150. [PubMed: 26371314]
29. Schweighoffer E, Nys J, Vanes L, Smithers N, Tybulewicz VLJ. TLR4 signals in B lymphocytes are transduced via the B cell antigen receptor and SYK. J Exp Med. 2017; 214:1269–1280. [PubMed: 28356391]
30. Manning BD, Toker A. AKT/PKB signaling: navigating the network. Cell. 2017; 169:381–405. [PubMed: 28431241]
31. Scharenberg AM, Humphries LA, Rawlings DJ. Calcium signalling and cell-fate choice in B cells. Nat Rev Immunol. 2007; 7:778–789. [PubMed: 17853903]

32. Okkenhaug K, et al. Impaired B and T cell antigen receptor signaling in p110δ PI 3-kinase mutant mice. Science. 2002; 297:1031–1034. [PubMed: 12130661]

33. Wang Y, et al. The physiologic role of CD19 cytoplasmic tyrosines. Immunity. 2002; 17:501–514. [PubMed: 12387743]

34. Sellars E, Gabra M, Salmena L. The complex landscape of PTEN mRNA regulation. Cold Spring Harb Perspect Med. 2020; 10 a036236 [PubMed: 31871240]

35. Dexheimer PJ, Cochella L. MicroRNAs: from mechanism to organism. Front Cell Dev Biol. 2020; 8:409. [PubMed: 32582699]

36. Reimao-Pinto MM, et al. Uridylation of RNA hairpins by Tailor confines the emergence of microRNAs in *Drosophila* . Mol Cell. 2015; 59:203–216. [PubMed: 26145176]

37. Agarwal V, Bell GW, Nam J-W, Bartel DP. Predicting effective microRNA target sites in mammalian mRNAs. eLife. 2015; 4 e05005

38. Xiao C, et al. Lymphoproliferative disease and autoimmunity in mice with increased miR-17-92 expression in lymphocytes. Nat Immunol. 2008; 9:405–414. [PubMed: 18327259]

39. Huse JT, et al. The PTEN-regulating microRNA miR-26a is amplified in high-grade glioma and facilitates gliomagenesis in vivo. Genes Dev. 2009; 23:1327–1337. [PubMed: 19487573]

40. Tumaneng K, et al. YAP mediates crosstalk between the Hippo and PI(3)K-TOR pathways by suppressing PTEN via miR-29. Nat Cell Biol. 2012; 14:1322–1329. [PubMed: 23143395]

41. Zou H, et al. MicroRNA-29A/PTEN pathway modulates neurite outgrowth in PC12 cells. Neuroscience. 2015; 291:289–300. [PubMed: 25665754]

42. Lin X, et al. MicroRNA-29 regulates high-glucose-induced apoptosis in human retinal pigment epithelial cells through PTEN. In Vitro Cell Dev Biol Anim. 2016; 52:419–426. [PubMed: 26822433]

43. Ji J, et al. Mitochondria-related miR-141-3p contributes to mitochondrial dysfunction in HFD-induced obesity by inhibiting PTEN. Sci Rep. 2015; 5 16262 [PubMed: 26548909]

44. Jin Y-Y, et al. Involvement of microRNA-141-3p in 5-fluorouracil and oxaliplatin chemo-resistance in esophageal cancer cells via regulation of PTEN. Mol Cell Biochem. 2016; 422:161–170. [PubMed: 27644195]

45. Li X-Y, et al. Triptolide restores autophagy to alleviate diabetic renal fibrosis through the miR-141-3p/PTEN/Akt/mTOR pathway. Mol Ther Nucleic Acids. 2017; 9:48–56. [PubMed: 29246323]

46. Papadopoulou AS, et al. The thymic epithelial microRNA network elevates the threshold for infection-associated thymic involution via miR-29a mediated suppression of the IFN-a receptor. Nat Immunol. 2011; 13:181–187. [PubMed: 22179202]

47. Dooley J, et al. The microRNA-29 family dictates the balance between homeostatic and pathological glucose handling in diabetes and obesity. Diabetes. 2016; 65:53–61. [PubMed: 26696639]

48. Anzelon AN, Wu H, Rickert RC. *Pten* inactivation alters peripheral B lymphocyte fate and reconstitutes CD19 function. Nat Immunol. 2003; 4:287–294. [PubMed: 12563260]

49. Suzuki A, et al. Critical roles of *Pten* in B cell homeostasis and immunoglobulin class switch recombination. J Exp Med. 2003; 197:657–667. [PubMed: 12615906]

50. Smeenk L, et al. Molecular role of the PAX5-ETV6 oncoprotein in promoting B-cell acute lymphoblastic leukemia. EMBO J. 2017; 36:718–735. [PubMed: 28219927]

51. Gonda H, et al. The balance between Pax5 and Id2 activities is the key to AID gene expression. J Exp Med. 2003; 198:1427–1437. [PubMed: 14581609]

52. Tran TH, et al. B cell-specific and stimulation-responsive enhancers derepress *Aicda* by overcoming the effects of silencers. Nat Immunol. 2010; 11:148–154. [PubMed: 19966806]

53. Omori SA, et al. Regulation of class-switch recombination and plasma cell differentiation by phosphatidylinositol 3-kinase signaling. Immunity. 2006; 25:545–557. [PubMed: 17000121]

54. Dengler HS, et al. Distinct functions for the transcription factor Foxo1 at various stages of B cell differentiation. Nat Immunol. 2008; 9:1388–1398. [PubMed: 18978794]

55. Medzhitov R, Horng T. Transcriptional control of the inflammatory response. Nat Rev Immunol. 2009; 9:692–703. [PubMed: 19859064]

56. Deane JA, Fruman DA. Phosphoinositide 3-kinase: diverse roles in immune cell activation. Annu Rev Immunol. 2004; 22:563–598. [PubMed: 15032589]
57. Fruman DA, et al. Impaired B cell development and proliferation in absence of phosphoinositide 3-kinase p85a. Science. 1999; 283:393–397. [PubMed: 9888855]
58. Suzuki H, et al. *Xid-like* immunodeficiency in mice with disruption of the p85a subunit of phosphoinositide 3-kinase. Science. 1999; 283:390–392. [PubMed: 9888854]
59. Rickert RC, Rajewsky K, Roes J. Impairment of T-cell-dependent B-cell responses and B-1 cell development in CD19-deficient mice. Nature. 1995; 376:352–355. [PubMed: 7543183]
60. Engel P, et al. Abnormal B lymphocyte development, activation, and differentiation in mice that lack or overexpress the CD19 signal transduction molecule. Immunity. 1995; 3:39–50. [PubMed: 7542548]
61. Martin F, Kearney JF. Positive selection from newly formed to marginal zone B cells depends on the rate of clonal production, CD19, and *btk* . Immunity. 2000; 12:39–49. [PubMed: 10661404]
62. Janas ML, et al. The effect of deleting p110d on the phenotype and function of PTEN-deficient B cells. J Immunol. 2008; 180:739–746. [PubMed: 18178811]
63. Calamito M, et al. Akt1 and Akt2 promote peripheral B-cell maturation and survival. Blood. 2010; 115:4043–4050. [PubMed: 20042722]
64. Srinivasan L, et al. PI3 kinase signals BCR-dependent mature B cell survival. Cell. 2009; 139:573–686. [PubMed: 19879843]
65. Hines MJ, et al. miR-29 sustains B cell survival and controls terminal differentiation via regulation of PI3K signaling. Cell reports. 2020; 33 108436 [PubMed: 33264610]
66. de Alboran IM, et al. Analysis of C-MYC function in normal cells via conditional gene-targeted mutation. Immunity. 2001; 14:45–55. [PubMed: 11163229]
67. Li S, et al. The transcription factors Egr2 and Egr3 are essential for the control of inflammation and antigen-induced proliferation of B and T cells. Immunity. 2012; 37:685–696. [PubMed: 23021953]
68. Goodnow CC, Vinuesa CG, Randall KL, Mackay F, Brink R. Control systems and decision making for antibody production. Nat Immunol. 2010; 11:681–688. [PubMed: 20644574]
69. Rolf J, et al. Phosphoinositide 3-kinase activity in T cells regulates the magnitude of the germinal center reaction. J Immunol. 2010; 185:4042–4052. [PubMed: 20826752]
70. Suzuki A, et al. T cell-specific loss of *Pten* leads to defects in central and peripheral tolerance. Immunity. 2001; 14:523–534. [PubMed: 11371355]
71. Harfe BD, McManus MT, Mansfield JH, Hornstein E, Tabin CJ. The RNaseIII enzyme Dicer is required for morphogenesis but not patterning of the vertebrate limb. Proc Natl Acad Sci USA. 2005; 102:10898–10903. [PubMed: 16040801]
72. Smith KG, Light A, Nossal GJ, Tarlinton DM. The extent of affinity maturation differs between the memory and antibody-forming cell compartments in the primary immune response. EMBO J. 1997; 16:2996–3006. [PubMed: 9214617]
73. Minnich M, et al. Multifunctional role of the transcription factor Blimp-1 in coordinating plasma cell differentiation. Nat Immunol. 2016; 17:331–343. [PubMed: 26779602]
74. Langmead B, Trapnell C, Pop M, Salzberg SL. Ultrafast and memory-efficient alignment of short DNA sequences to the human genome. Genome Biol. 2009; 10 R25 [PubMed: 19261174]
75. Zhang Y, et al. Model-based analysis of ChIP-Seq (MACS). Genome Biol. 2008; 9 R137 [PubMed: 18798982]
76. Anders S, Pyl PT, Huber W. HTSeq-a Python framework to work with high-throughput sequencing data. Bioinformatics. 2015; 31:166–169. [PubMed: 25260700]
77. Love MI, Huber W, Anders S. Moderated estimation of fold change and dispersion for RNA-seq data with DESeq2. Genome Biol. 2014; 15:550. [PubMed: 25516281]
78. Alberti C, et al. Cell-type specific sequencing of microRNAs from complex animal tissues. Nat Methods. 2018; 15:283–289. [PubMed: 29481550]
79. Kozomara A, Birgaoanu M, Griffiths-Jones S. miRBase: from microRNA sequences to function. Nucleic Acids Res. 2019; 47:D155–D162. [PubMed: 30423142]

Europe PMC Funders Author Manuscripts

80. Adams B, et al. *Pax-5* encodes the transcription factor BSAP and is expressed in B lymphocytes, the developing CNS, and adult testis. Genes Dev. 1992; 6:1589–1607. [PubMed: 1516825]
81. öhner M, et al. Molecular functions of the transcription factors E2A and E2-2 in controlling germinal center B cell and plasma cell development. J Exp Med. 2016; 213:1201–1221. [PubMed: 27261530]
82. Yates A, et al. Ensembl 2016. Nucleic Acids Res. 2016; 44:D710–D716. [PubMed: 26687719]
83. Thijs G, et al. A Gibbs sampling method to detect overrepresented motifs in the upstream regions of coexpressed genes. J Computational Biol. 2002; 9:447–464.
84. Rice P, Longden I, Bleasby A. EMBOSS: the European Molecular Biology Open Software Suite. Trends in genetics : TIG. 2000; 16:276–277. [PubMed: 10827456]
85. Kieffer-Kwon KR, et al. Interactome maps of mouse gene regulatory domains reveal basic principles of transcriptional regulation. Cell. 2013; 155:1507–1520. [PubMed: 24360274]
86. Luo W, et al. The AKT kinase signaling network is rewired by PTEN to control proximal BCR signaling in germinal center B cells. Nat Immunol. 2019; 20:736–746. [PubMed: 31011187]

One Sentence Summary

Pax5 controls the generation, proliferation and survival of all mature B cells by promoting PI3K signaling via PTEN downregulation.

Europe PMC Funders Author Manuscripts

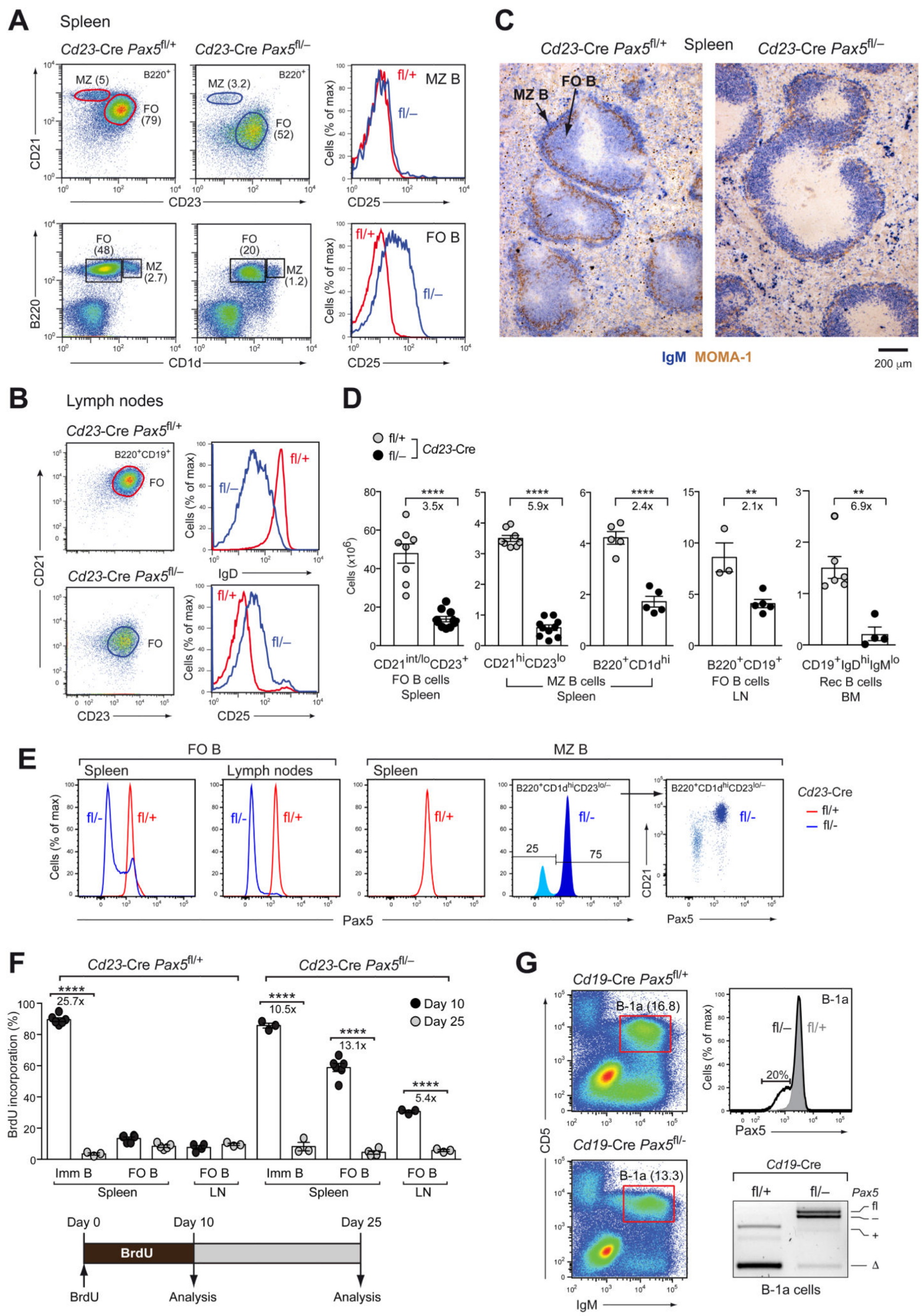

Figure 1. Loss of mature B cell types upon *Pax5* inactivation.

(**A,B**) Flow-cytometric analysis of MZ B ($B220^{+}CD21^{hi}CD23^{lo/-}$) and FO B ($B220^{+}CD21^{int/lo}CD23^{hi}$) cells from the spleen (**A**) and FO B cells from lymph nodes (B) of *Cd23*-Cre *Pax5* $^{fl/-}$ (fl/–) and *Cd23*-Cre *Pax5* $^{fl/+}$ (fl/$^{+}$) mice. The percentages of cells in each gate are indicated. (**C**) Staining of spleen sections for MOMA-1 (brown) and IgM (blue) expression. (**D**) Absolute numbers of the indicated cell types in the spleen, lymph nodes (LN) and bone marrow (BM) of *Cd23*-Cre *Pax5* $^{fl/+}$ mice (gray dots) and *Cd23*-Cre *Pax5* $^{fl/-}$ mice (black dots). (**E**) Intracellular Pax5 staining of FO B and MZ B ($CD19^{+}B220^{+}$CD

1d^{hi}CD23$^{lo/−}$) cells. (**F**) BrdU labeling of splenic immature and FO B cells and lymph node FO B cells of 2-month-old *Cd23*-Cre *Pax5* $^{fl/+}$ and *Cd23*-Cre *Pax5* $^{fl/−}$ mice. BrdU^{+} B cells were identified by flow cytometry after 10 days of BrdU labeling (black dots) or after a subsequent 15-day chase period (gray dots) without BrdU in the drinking water (Fig. S1C), as shown by the diagram below. (**G**) Flow-cytometric analysis of B-1a cells (IgM^{hi}CD5^{+}) from the peritoneum of *Cd19*-Cre *Pax5* $^{fl/−}$ (fl/–; black) and *Cd19*-Cre *Pax5* $^{fl/+}$ (fl/$^{+}$; gray) mice. Upper right: Intracellular Pax5 staining of B-1a cells. The percentage of *Cd19*-Cre *Pax5* $^{fl/−}$ B-1a cells with reduced Pax5 expression is shown. Lower right: PCR analysis of the deletion of the floxed *Pax5* allele in B-1a cells (IgM^{hi}CD5^{+}). PCR fragments corresponding to the deleted (Δ) or intact (fl) floxed *Pax5* allele and the wild-type (+) or null (–) *Pax5* allele are indicated. Statistical data (**D**, **F**) are shown as mean value with SEM and were analyzed by two-tailed unpaired Student's *t*-test (**D**) or two-way ANOVA with Šídák's multiple comparison test (**F**); **$P < 0.01$, ****$P < 0.0001$. Each dot represents one mouse.

Europe PMC Funders Author Manuscripts

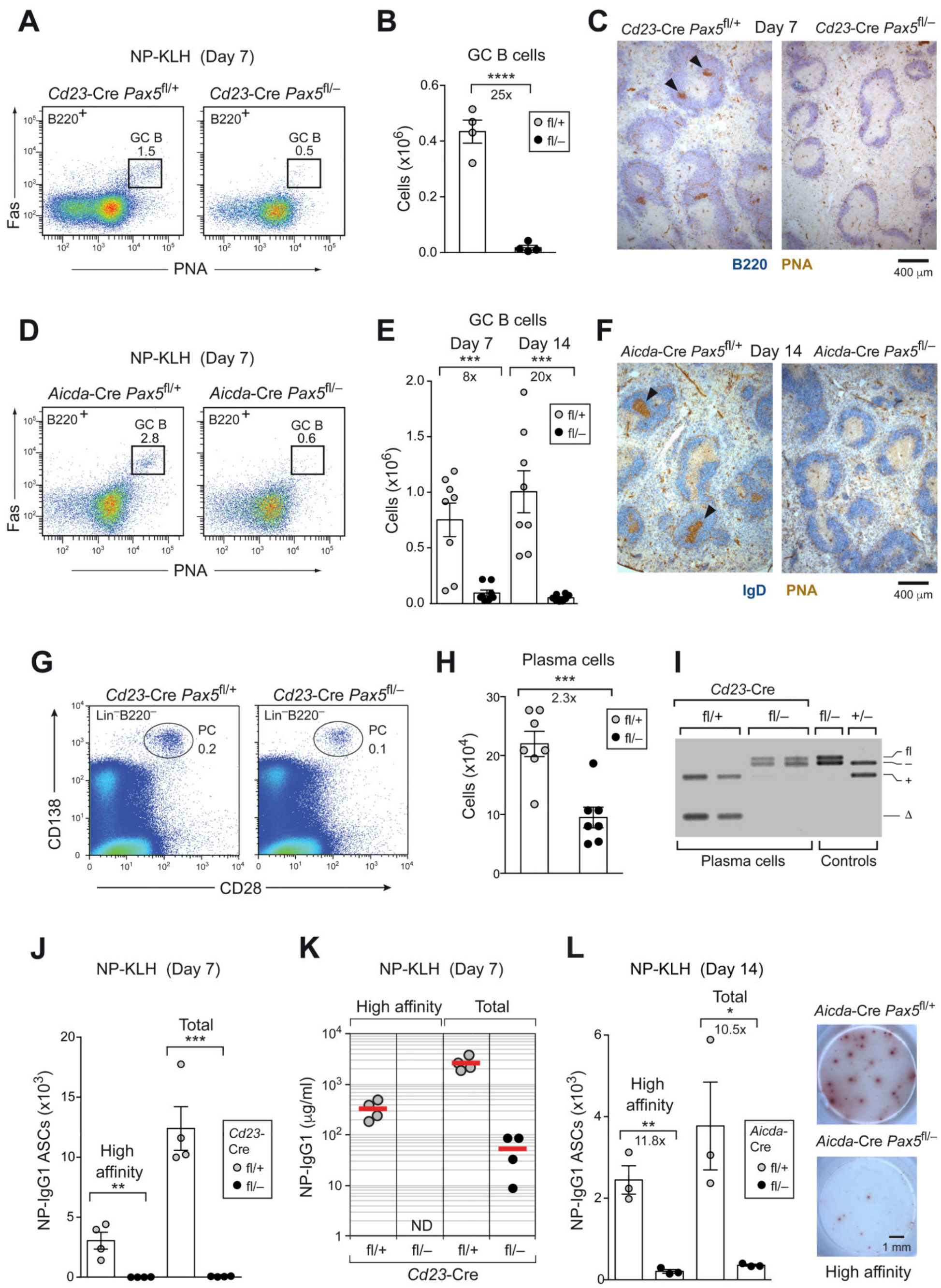

Figure 2. The initiation and maintenance of GC B cell differentiation depended on Pax5.
(**A-C**) GC B cell differentiation in the spleen of *Cd23*-Cre *Pax5* $^{fl/+}$ (fl/$^{+}$; gray dots) and *Cd23*-Cre *Pax5* $^{fl/–}$ (fl/–; black dots) mice at day 7 after immunization with NP-KLH (in alum). Absolute numbers of GC B cells (B220^{+}Fas^{+}PNA^{+}) were determined by flow cytometry (**A,B**), and PNA^{+} GC B cells were visualized by staining of spleen sections for PNA (brown) and B220 (blue) expression (**C**). Arrowheads indicate GCs. (**D-F**) GC B cell differentiation in the spleen of *Aicda*-Cre *Pax5* $^{fl/+}$ and *Aicda*-Cre *Pax5* $^{fl/–}$ mice at day 7 and 14 after immunization with NP-KLH (in alum) was analyzed, as described above. (**G-I**)

Flow-cytometric analysis of plasma cells ($CD28^{+}CD138^{+}Lin^{-}$) from the bone marrow (femur and tibia of hind legs) of non-immunized *Cd23*-Cre *Pax5* $^{fl/+}$ and *Cd23*-Cre *Pax5* $^{fl/-}$ mice (**G,H**). PCR determination of *Pax5* exon 2 deletion in sorted plasma cells (**I**), as described in Fig. 1G. (**J-L**) T cell-dependent immune responses. *Pax5* $^{fl/+}$ and *Pax5* $^{fl/-}$ mice carrying *Cd23*-Cre (**J**) or *Aicda*-Cre (**L**) were immunized with NP-KLH (in alum) and analyzed at the indicated days after immunization by ELISPOT assay to determine NP-specific IgG1 antibody-secreting cells (ASCs) in the spleen. NP4-BSA- or NP_{23}-BSA-coated plates were used for detecting ASCs secreting high-affinity or total anti-NP-IgG1 antibodies, respectively. Representative ELISPOT images are shown. (**K**) ELISA analysis of serum titers of NP-specific IgG1 antibodies using NP7-BSA- or NP_{30}-BSA-coated plates. ND, not detected. Statistical data (**B,E,H,J,L**) are shown as mean value with SEM and were analyzed by the two-tailed unpaired Student's *t*-test; *$P < 0.05$; ***$P < 0.001$ and ****$P < 0.0001$. Each dot represents one mouse.

Europe PMC Funders Author Manuscripts

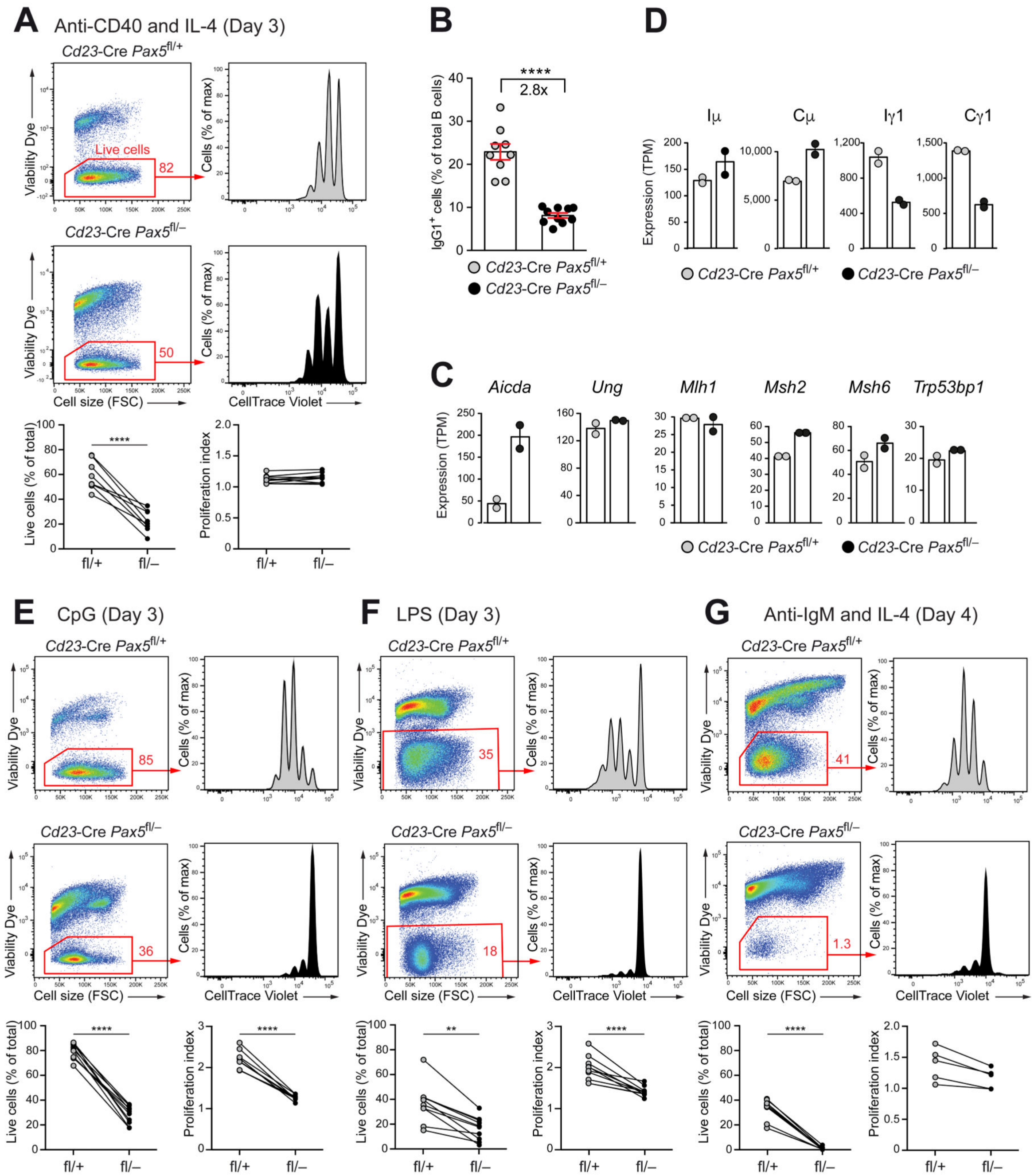

Figure 3. Pax5 controlled B cell proliferation in response to BCR and TLR signaling.

(**A,B**) Proliferation and IgG1 CSR response to anti-CD40 plus IL-4 stimulation. CellTrace Violet-labeled FO B cells from lymph nodes of *Cd23*-Cre *Pax5* $^{fl/-}$ (fl/–; black) and *Cd23*-Cre *Pax5* $^{fl/+}$ (fl/+; gray) mice were stimulated with anti-CD40 and IL-4 for 3 (**A**) or 4 (**B**) days and then stained with the Viability Dye eFluor™ 780. The cell viability and proliferation index of the stimulated cells (**A**) and the percentage of IgG1^{+} B cells (**B**) were determined by flow-cytometric analysis. Lines connect the results obtained with Pax5-deficient and control B cells in the same stimulation experiment. (**C,D**) Gene expression in

Europe PMC Funders Author Manuscripts

lymph node B cells stimulated with anti-CD40 and IL-4 for 2 days, as determined by RNA-seq (Fig. S3E). The expression of selected genes involved in CSR (**C**) and the abundance of germline transcripts at the Iμ and Ig1 exons and transcripts at the Cμ and Cg1 exons (**D**) are shown as mean expression value (TPM, transcripts per million) with SEM based on two independent RNA-seq experiments per genotype. (**E-G**) Stimulation of lymph node FO B cells of the indicated genotypes with CpG oligodeoxynucleotides (**E**) and LPS (**F**) for 3 days or with anti-IgM and IL-4 (**G**) for 4 days, as described (**A**). The data (**A,E,F,G**) were statistically analyzed by the two-tailed unpaired Student's test: $^{**}P < 0.01$, $^{****}P < 0.0001$. Each dot represents one mouse.

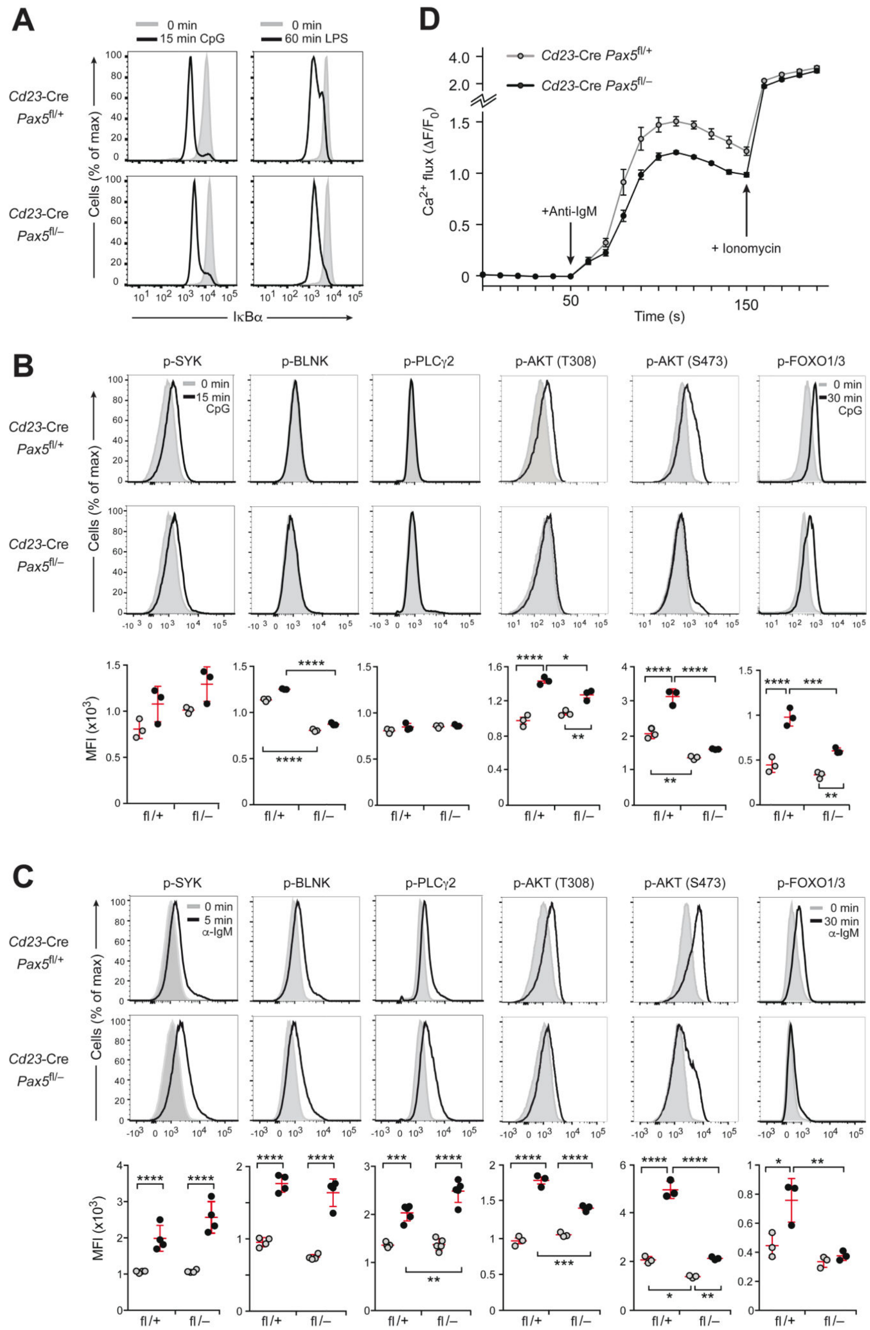

Figure 4. Intracellular signaling upon TLR9 and BCR activation in Pax5-deficient FO B cells.

(**A**) IκBα degradation upon TLR signaling. The IkBa protein amount was determined by intracellular staining of CD43^{-} FO B cells from lymph nodes of *Cd23*-Cre *Pax5* $^{fl/-}$ or control *Cd23*-Cre *Pax5* $^{fl/+}$ mice before (gray surface) and after (black line) stimulation for 15 min with CpG oligodeoxynucleotides or for 60 min with LPS. (**B,C**) Intracellular TLR9 and BCR signaling. The phosphorylation (p-) status of signal transducers of the calcium and PI3K signaling pathways (Fig. S4A) was determined in lymph node FO B cells of the indicated genotypes before or after stimulation with CpG oligodeoxynucleotides for 15 min

(**B**) or stimulation with anti-IgM for 5 min (**C**) except for a 30-min stimulation with either stimuli for analyzing p-FOXO1,3. (**B,C**). Flow cytometry (top and middle) was performed with antibodies specific for p-AKT (p-Thr308) p-AKT (p-Ser473), p-BLNK (p-Tyr84), p-PLC**γ**2 (p-Tyr759), p-SYK (p-Tyr525/526) and p-FOXO1 (p-Thr24)/p-FOXO3 (p-Thr32). Bottom, the median fluorescence intensity (MFI) for untreated (gray dots) and stimulated (black dots) FO B cells of the indicated genotypes is shown. Statistical data are indicated as mean value with SEM and were analyzed by two-way ANOVA with Tukey's multiple comparison test; *$P < 0.05$, **$P < 0.01$, ***$P < 0.001$, ****$P < 0.0001$. Each dot represents one mouse. One of at least three experiments is shown. (**D**) Calcium mobilization in response to BCR signaling. Intracellular Ca^{2+} fluxes in $CD43^{-}$ FO B cells from lymph nodes of the indicated genotypes were recorded as an increase of the fluorescent emission of a Ca^{2+} sensor dye after addition of anti-IgM (arrow, after 50 s) or ionomycin (arrow, after 150 s) and are presented as $\Delta F/F_0$ (F_0, average fluorescence before antibody addition; ΔF, fluorescence at time 't' - F_0). Mean values with SEM are shown for 3 independent experiments.

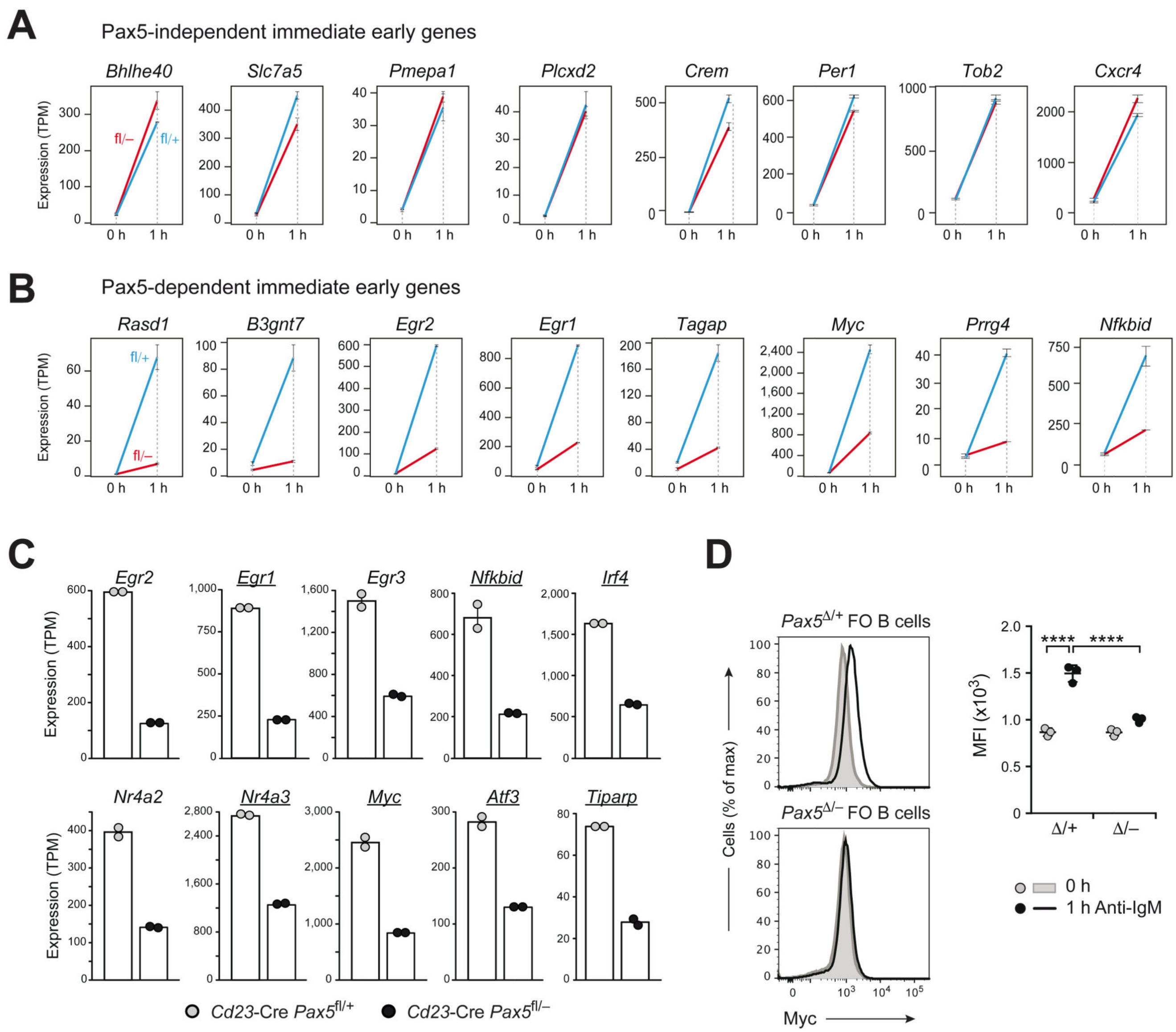

Figure 5. Activation of immediate-early genes in response to BCR signaling.

(**A,B**) Pax5-independent (**A**) and Pax5-dependent (**B**) immediate-early genes that were induced > 9-fold upon anti-IgM stimulation in control FO B cells and were further defined, as described in Fig. S5D-F and the Materials and Methods. The expression of activated genes in *Cd23*-Cre *Pax5* $^{fl/+}$ (fl/+; blue) and *Cd23*-Cre *Pax5* $^{fl/-}$ (fl/–; red) FO B cells before (0 h) and after (1 h) of anti-IgM stimulation is shown as mean expression value (TPM) with SEM based on two independent RNA-seq experiments for each genotype and treatment condition. (**C**) mRNA expression of Pax5-dependent immediate-early genes, coding for known transcription factors, is shown for FO B cells of the indicated genotypes after 1 h of anti-IgM stimulation. Genes bound by Pax5 (12) are underlined. (**D**) Intracellular Myc staining of *Cd23*-Cre *Pax5* $^{fl/+}$ (*Pax5* $^{\Delta/+}$) and *Cd23*-Cre *Pax5* $^{fl/-}$ (*Pax5* $^{\Delta/-}$) FO B cells before (gray) and after (black) stimulation for 1 h with anti-IgM (left). Myc expression (right) is shown as mean MFI value with SEM and was analyzed by twoway ANOVA with Tukey's multiple comparison test; ****$P < 0.0001$. Each dot represents one mouse.

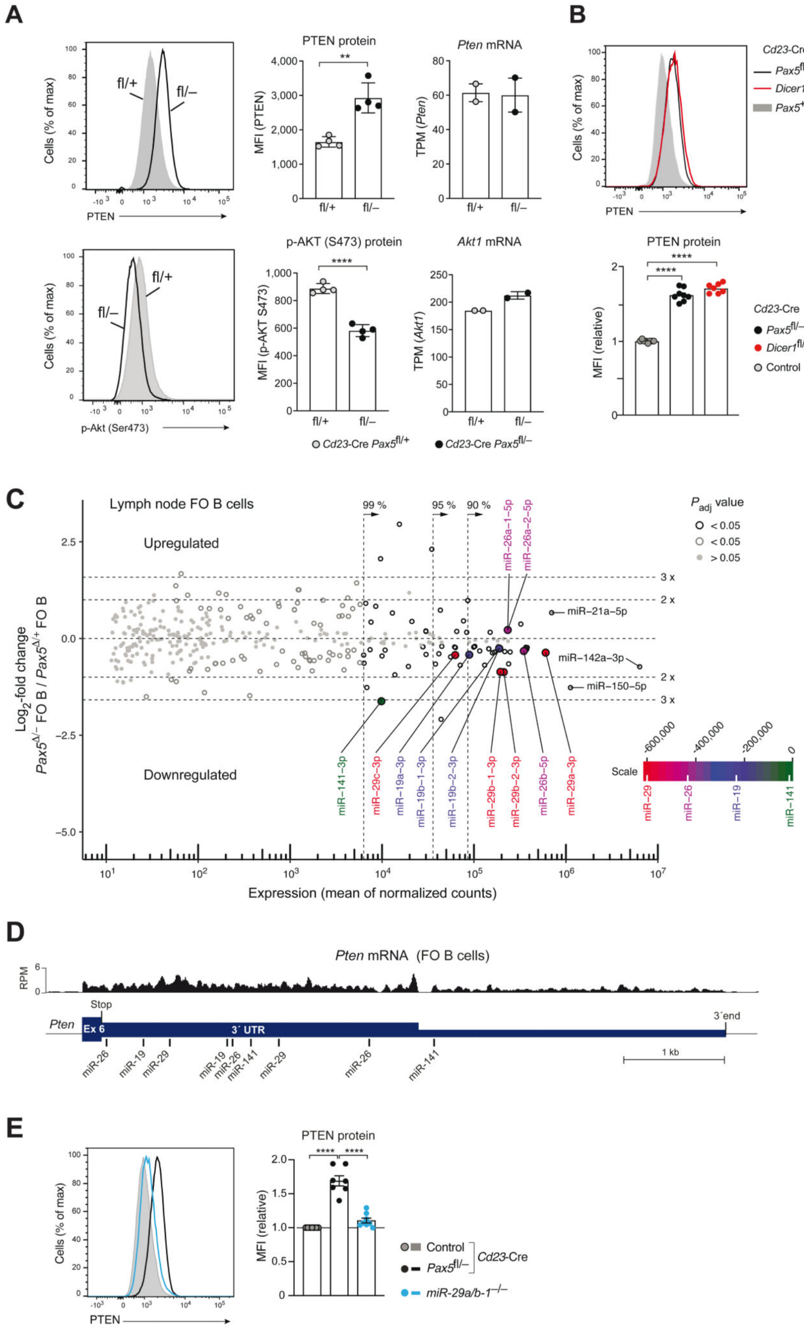

Figure 6. Pax5 downregulated PTEN expression by controlling the abundance of *Pten*-targeting microRNAs.

(**A**) PTEN protein expression and phosphorylation of AKT (Ser473) in unstimulated lymph node FO B cells of *Cd23*-Cre *Pax5* $^{fl/−}$ (back) and *Cd23*-Cre *Pax5* $^{fl/+}$ (gray) mice, as determined by intracellular staining (left) and MFI quantification (middle). *Pten* and *Akt1* mRNA expression in the same FO B cell types (right) is shown as mean expression value (TPM) with SEM, as determined by RNA-seq. (**B**) PTEN expression in lymph node FO B cells of *Cd23*-Cre *Dicer1* $^{fl/fl}$ (red), *Cd23*-Cre *Pax5* $^{fl/−}$ (black) and *Cd23*-Cre *Pax5* $^{+/+}$ (gray) mice, as determined by intracellular staining and quantification of the MFI values relative to the control genotypes (*Cd23*-Cre *Pax5* $^{+/+}$ *Dicer1* $^{+/+}$, *P*ax5$^{+/+}$ *Dicer1* $^{+/+}$, *Pax5* $^{fl/+}$ *Dicer1* $^{+/+}$, *Pax5* $^{+/+}$ *Dicer1* $^{fl/+}$ or *P*ax5$^{+/+}$ *Dicer1* $^{fl/fl}$). (C) MA plot of miRNA expression differences between *Cd23*-Cre *Pax5* $^{fl/-}$ (*Pax5* $^{\Delta/-}$) and *Cd23*-Cre *Pax5* $^{fl/+}$ (*Pax5* $^{\Delta/+}$) FO B cells, which were isolated from lymph nodes as CD23^{+} cells by immunomagnetic sorting. Two small-RNA-seq experiments per genotype were performed. The abundance of individual miRNAs in the two B cell types is plotted as mean value of the normalized counts versus the log2-fold change in abundance between *Pax5* $^{\Delta/-}$ and *Pax5* $^{\Delta/+}$ FO B cells (Table S4 and S6). Dotted lines indicate the area containing 99%, 95% or 90% of the total normalized counts. The statistical significance of the observed differences is indicated by gray and black circles (P value < 0.05) or gray dots (P value > 0.05). Adjusted P values were determined by DESeq2. Each symbol represents one miRNA species. *Pten*-targeting miRNAs are highlighted by the color corresponding to their position on the scale bar, which was generated by multiplying the sum of the normalized read counts of all members of a miRNA family with the total context+/+ score of the miRNA family (Table S5). (**D**) Location of the target sites of the indicated miRNAs in the 3'UTR of the mouse *Pten* mRNA, as predicted by the TargetScanMouse algorithm (v7.2; targetscan.org; (37)). The mRNA-seq profile of *Pten* exon 6 in control FO B cells is shown. (**E**) PTEN expression in unstimulated lymph node FO B cells of *miR-29a/b-1* $^{-/-}$ (blue), *Cd23*-Cre *Pax5* $^{fl/-}$ (back) and control *Cd23*-Cre *Pax5* $^{fl/+}$ (gray) mice, as determined by intracellular staining (left) and quantification of the MFI values (right) relative to control FO B cells (*Cd23*-Cre *Pax5* $^{+/+}$, *Cd23*-Cre *Pax5* $^{fl/+}$, *Pax5* $^{+/+}$ or *Pax5* $^{fl/fl}$). Statistical data (**A,B,E**) are shown as mean value with SEM and were statistically analyzed by the two-tailed unpaired Student's *t*-test (**A**) or by one-way ANOVA with Tukey's multiple comparison test (**B,E**): ** $P < 0.01$, **** $P < 0.0001$.

Europe PMC Funders Author Manuscripts

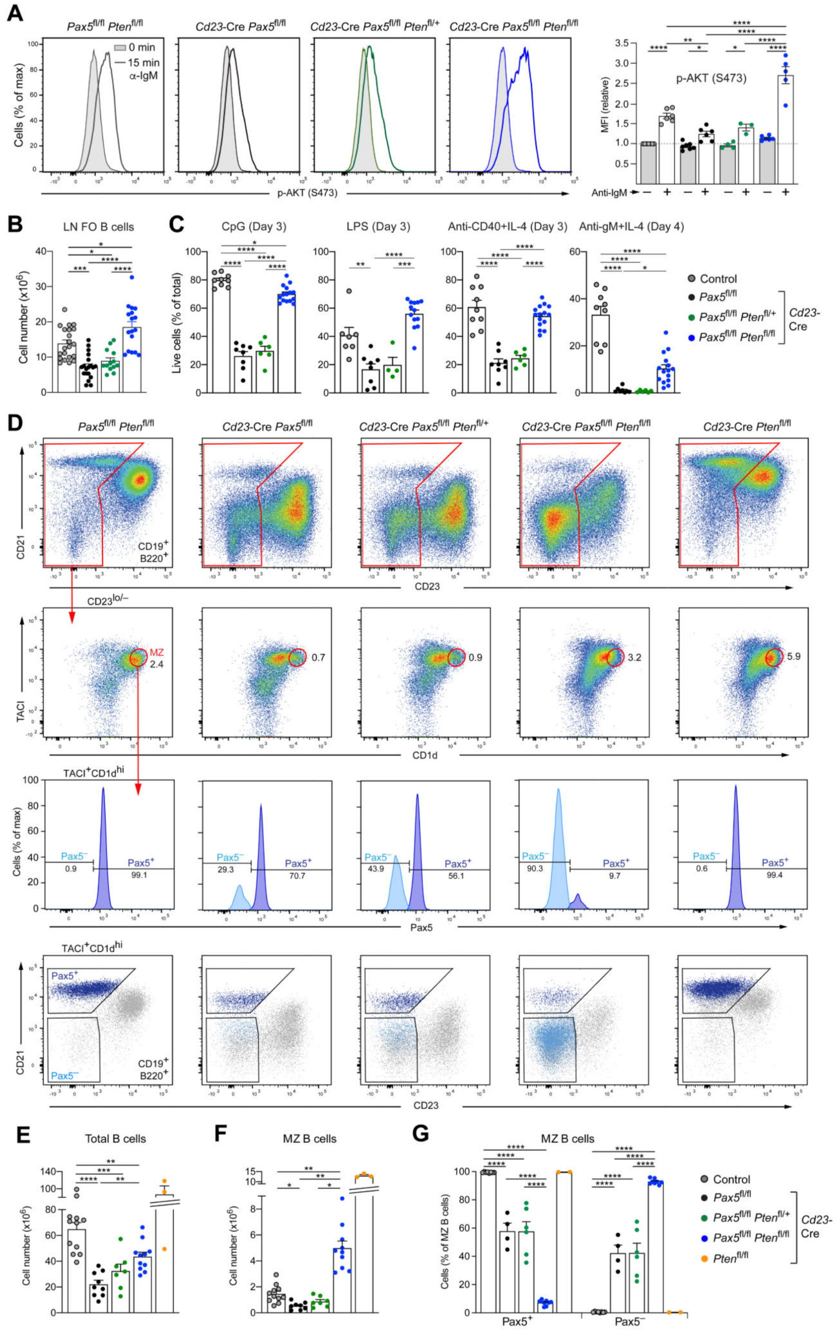

Figure 7. Loss of PTEN rescued PI3K signaling, FO B and MZ B cell numbers in *Pax5* mutant mice.

(**A**) Rescue of PI3K signaling. CD43^{-} FO B cells from lymph nodes of *Cd23*-Cre *Pax5* $^{fl/fl}$ (black), *Cd23*-Cre *Pax5* $^{fl/fl}$ *Pten* $^{fl/+}$ (green), *Cd23*-Cre *Pax5* $^{fl/fl}$ *Pten* $^{fl/fl}$ (blue) and control *Pax5* $^{fl/fl}$ *Pten* $^{fl/fl}$ (gray) mice were either left untreated (gray surface) or stimulated (colored line) for 15 min with anti-IgM prior to intracellular staining with an anti p-AKT (Ser473) antibody (left). Quantification of the MFI values relative to the unstimulated FO B cells of the control genotype is shown to the right. (**B,C**) Rescue of the FO B cell survival before and after stimulation. FO B cells from lymph nodes (LN) of the indicated genotypes were analyzed directly *ex vivo* (**B**) or after stimulation (**C**) with CpG oligodeoxynucleotides, LPS, anti-CD40 and IL-4 or anti-IgM and IL-4 for the indicated days prior to staining with the Viability Dye eFluor™ 780. The frequency of viable B cells is plotted. (**D**) Flow-cytometric analysis of MZ B cells in the spleen of the indicated genotypes. MZ B cells were identified as $CD19^{+}B220^{+}CD23^{lo/-}TACI^{+}CD1d^{hi}$ cells and analyzed for Pax5 protein expression by intracellular staining. As shown by backgating, the $Pax5^{+}$ MZ B cells expressed CD21, whereas the $Pax5^{-}$ MZ B cells lost CD21 expression. (**E-G**) Statistical analysis indicating the number of total B cells (**E**) and MZ B cells (**F**) as well as the relative frequency of $Pax5^{+}$ and $Pax5^{-}$ MZ B cells (**G**) in the spleen of mice of the five indicated genotypes. Statistical data are shown as mean value with SEM and were analyzed by two-way ANOVA with Šídák's multiple comparison test (**A**) or one-way (**B,C,E,F**) or two-way (**G**) ANOVA with Tukey's multiple comparison test; $*P < 0.05$, $**P < 0.01$, $***P < 0.001$, $****P < 0.0001$. Each dot represents one mouse. The control genotypes (**A,B,E,F,G**) were *Pax5* $^{fl/fl}$ *Pten* $^{fl/fl}$, *Pax5* $^{fl/fl}$ *Pten* $^{fl/+}$, *Pax5* $^{fl/fl}$ *Pten* $^{+/+}$ or *Cd23*-Cre *Pax5* $^{fl/+}$ *Pten* $^{+/+}$.

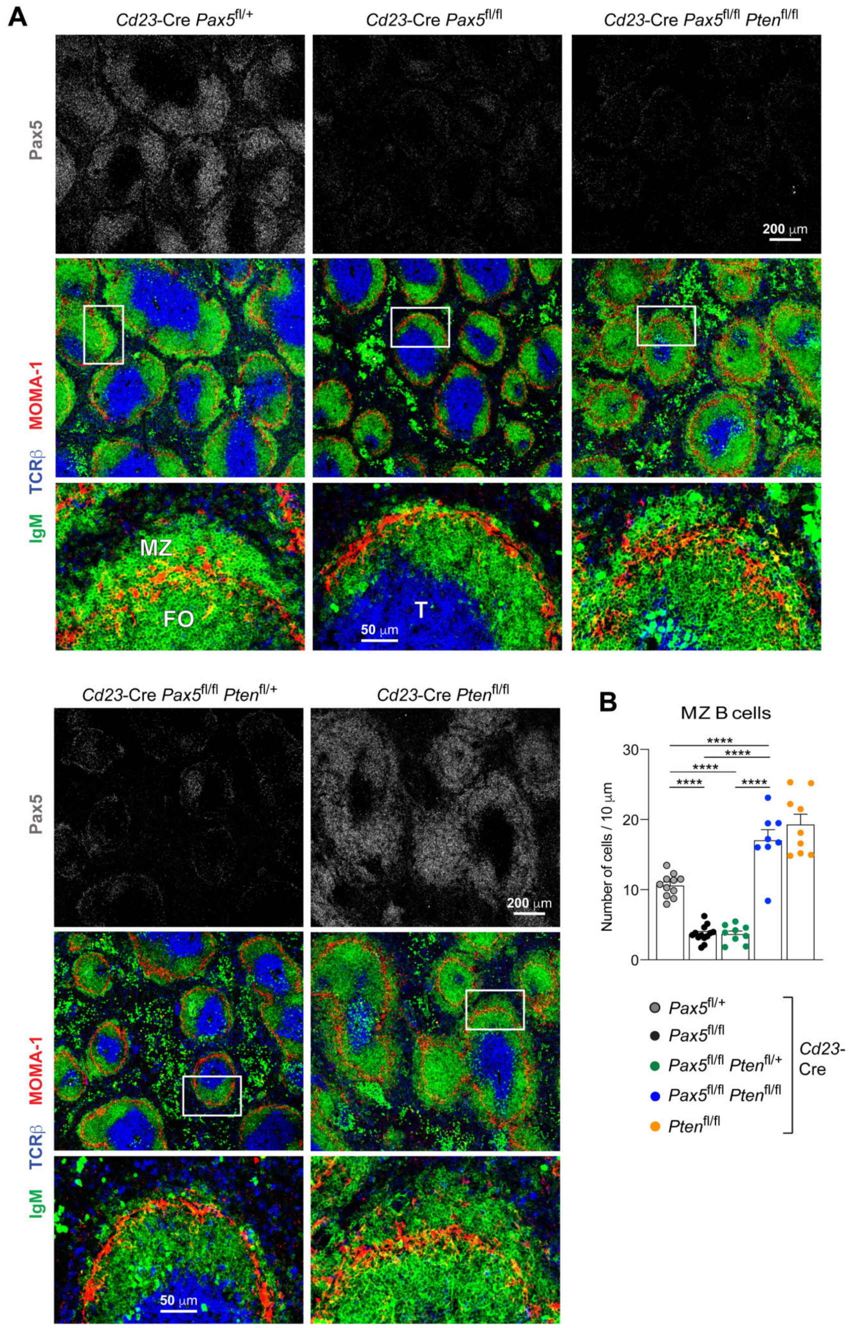

Figure 8. Rescue of MZ B cell development in *Pten,Pax5* double-mutant mice.

(**A**) Immunohistological analysis of spleen sections from 12-week-old mice of the indicated genotypes. The sections were stained with antibodies detecting IgM (green), MOMA-1 (red), TCRβ (blue) and Pax5 (gray). Selected areas (boxed) of B cell follicles are shown at higher magnification. T, FO B and MZ B cell zones are indicated. One of three experiments is shown. (**B**) Quantification of the MZ B cells on histological sections. The average number of IgM$^+$ B cells outside of the MOMA-1$^+$ macrophage ring was determined per 10 µm length of the perimeter of the MOMA-1$^+$ ring (see Methods). Each dot represents the measurement of one follicle. The mean values determined for the indicated genotypes is shown with SEM and were analyzed by one-way ANOVA with Tukey's multiple comparison test; ****$P < 0.0001$.

Europe PMC Funders Author Manuscripts